AD_____

Award Number: DAMD17-02-1-0573

TITLE: The Role of Phosphorylation in the Regulation of p27 Function in Breast Cancer

PRINCIPAL INVESTIGATOR: Michael K. Connor, Ph.D.
Mentor: Joyce M. Slingerland, M.D., Ph.D.

CONTRACTING ORGANIZATION: Sunnybrook & Women's College
Health Sciences Center
Toronto, Ontario Canada M4N 3M5

REPORT DATE: May 2003

TYPE OF REPORT: Annual Summary

PREPARED FOR: U.S. Army Medical Research and Materiel Command
Fort Detrick, Maryland 21702-5012

REPORT DOCUMENTATION PAGE

Form Approved
OMB No. 074-0188

1. AGENCY USE ONLY (Leave blank)	2. REPORT DATE	3. REPORT TYPE AND DATES COVERED
	May 2003	Annual Summary (1 May 2002 - 30 Apr 2003)

4. TITLE AND SUBTITLE
The Role of Phosphorylation in the Regulation of p27 Function in Breast Cancer

5. FUNDING NUMBERS
DAMD17-02-1-0573

6. AUTHOR(S)
Michael K. Connor, Ph.D.
Mentor: Joyce M. Slingerland, M.D., Ph.D.

7. PERFORMING ORGANIZATION NAME(S) AND ADDRESS(ES)
Sunnybrook & Women's College Health Sciences Center
Toronto, Ontario Canada M4N 3M5

E-Mail: michael.connor@swchsc.on.ca

8. PERFORMING ORGANIZATION REPORT NUMBER

9. SPONSORING / MONITORING AGENCY NAME(S) AND ADDRESS(ES)
U.S. Army Medical Research and Materiel Command
Fort Detrick, Maryland 21702-5012

10. SPONSORING / MONITORING AGENCY REPORT NUMBER

11. SUPPLEMENTARY NOTES
Original contains color plates: All DTIC reproductions will be in black and white.

12a. DISTRIBUTION / AVAILABILITY STATEMENT
Approved for Public Release; Distribution Unlimited

12b. DISTRIBUTION CODE

13. ABSTRACT (Maximum 200 Words)

Breast Cancer is a tragic disease that affects an increasing number of North American women each year. Although much is known about the disease, it appears this knowledge merely touches the surface of the mechanisms which underlie disease progression, often leading to patient death. Loss of the cell cycle inhibitor p27 in Breast Cancer Cells is known to be associated with advanced stage disease progression and poor patient prognosis. However, the mechanisms regulating the loss of p27 are only beginning to be understood. This proposal addresses the role of p27 phosphorylation on regulating p27 degradation. We find that the mitogen activated protein kinase (MAPK) pathway can lead to accelerated p27 degradation and a reduced protein half-life. Furthermore, MAPK activation alters p27 phosphorylation and increases p27 nuclear export. Opposite effects on p27 are observed when the MAPK pathway is inhibited by the drug U0126. This indicates the importance of this pathway in mediating p27 loss. Further work is being conducted to precisely determine the sites on p27 which are phosphorylated by MAPK which will lead to a better understanding of the potential mechanisms mediating p27 loss in Breast Cancer. The hope is that these results will lead to new therapeutic drug discovery.

14. SUBJECT TERMS
p27, nuclear export, MAP kinase, degradation

15. NUMBER OF PAGES
37

16. PRICE CODE

17. SECURITY CLASSIFICATION OF REPORT	18. SECURITY CLASSIFICATION OF THIS PAGE	19. SECURITY CLASSIFICATION OF ABSTRACT	20. LIMITATION OF ABSTRACT
Unclassified	Unclassified	Unclassified	Unlimited

Table of Contents

Introduction

Disregulation of the cell cycle is one of the hallmarks of cancer progression (13). Since the cdk inhibitor p27 plays such a vital role in regulating the cell cycle (11,12), it is not surprising that loss of p27 protein correlates with advanced cancer status and poor patient prognosis in many cancers, including breast cancer (3,9,13,15). To date, no mutations or deletions of the p27 gene have been reported, thus this loss of p27 protein is mediated by alterations in the expression of the native p27 gene. Research has suggested that loss of p27 is independent of both p27 transcription and p27 protein synthesis, but relies on accelerated p27 proteolysis (2,10,16,17). Much work has been done attempting to unfold the mysteries that underlie this disproportionate p27 degradation. New discoveries are continuing to expand the current theories and potentially pinpoint the precise alterations in p27 expression responsible for the loss of protein and the resultant breast cancer progression. We, and others, have recently reported a novel pathway of p27 degradation that occurs in G1, is independent of phosphorylation of p27 on threonine 187 (T187) by cdk 2 and occurs in the cytoplasm (5). This pathway depends on the phosphorylation of p27 on serine 10 (S10) and the subsequent export of p27 out of the nucleus into the cytoplasm (5,7). It also appears that dephosphorylation of S10 by an as yet unidentified phosphatase is necessary for the degradation of p27 within the cytoplasm. Acceleration of this nuclear export-dependent mechanism of p27 proteolysis would result in a reduction in cellular p27 levels during G1, would promote the transition into S-phase and subsequently activate cyclin E/cdk 2-mediated p27 degradation. Thus, it appears that although this export-dependent degradation only accounts for a minor portion of the total p27 proteolysis, it is very important in activating the established cyclin E/cdk 2-dependent degradation mechanisms.

Body

Following the submission, acceptance and instatement of my post-doctoral traineeship, certain factors resulted in alterations to the approved statement of work. At the Cold Spring Harbor Cell Cycle Meeting in April 2002, two groups presented work outlining their discovery of the E3 ubiquitin ligase responsible for p27 degradation in the cytoplasm in G1. Also, my mentor Dr. Joyce Slingerland accepted a position as the

director of the Sylvester Cancer Center at the University of Miami, which was effective August 15, 2002. As such I have been forced to drastically alter my statement of work. In addition, I have begun working in the lab of a new mentor Dr. Arun Seth here at Sunnybrook & Women's College Health Sciences Centre as of September, 2002. I will not present any of the results that I have obtained in Dr. Seth's lab. I feel it would confuse the issue and detract from the data obtained that is relevant to my original statement of work. Thus, my original statement of work has been altered in the following ways. I have decided to forgo Aim 2 as I am at a decided competitive disadvantage based on the results presented at the last Cold Spring Harbor Cell Cycle meeting. Thus, I have decided to combine aims 1 and 3 and pursue the role of the MAP kinase pathway in mediating p27 degradation. I have been given permission to change mentors and will submit an updated statement of work to reflect this change.

It has been published that p27 levels are reduced in response to activation of the MAP kinase pathway (6,18). However, as with other aspects of p27 function, there appears to be a question as to whether this is the case in all cell types (4). I have chosen to use malignant MCF-7 human mammary epithelial cells to study the potential role of MAP kinase on p27 degradation in a breast cancer environment. Studies using mouse fibroblasts (NIH 3T3) showed no reduction in p27 after increased MAP kinase activation, which contradicts observations in other cell types (4). We have also observed differences in p27 regulation in MCF-7 cells compared to published results in NIH 3T3 cells, specifically with regard to the stability of S10A mutant p27 (5,7). We feel this is a result of an inherent way that p27 is regulated in mouse cells versus human mammary epithelial cells. There is precedence for this, as mouse p27 lacks threonine 157 (T157), which is an important site for the regulation of p27 in human cells. We initially attempted to generate MCF-7 cells that inducibly express MEK^{EE}, a constitutively active MEK. After characterizing approximately 35 clones we were unsuccessful in obtaining any inducible MEK^{EE} clones. Thus we decided to use transient transfections of the MEK^{EE} expression vectors to activate the MAP kinase pathway. Using 1 μg of DNA I was able to dramatically increase the levels of MEK, resulting in an increased phosphorylation of MAPK (Fig. 1A). Upon expression of MEK^{EE} the levels of p27 are reduced to barely detectable levels. In addition, activation of the MAP kinase pathway altered moved p27

into cyclin D1-bound complexes, as shown by immunoprecipitation of p27 from asynchronously growing cells in the presence or absence of MEK^{EE} (Fig. 1 B). Furthermore, this reduction in p27 levels is a result of an increased degradation of p27 following transfection of MEK^{EE} (Fig. 1C). Cells were labeled with ^{35}S-methionine for 30 minutes and harvested from 1-8 hours after removal of the ^{35}S. The half-life of p27 in the absence of MEK^{EE} is between 4 and 8 hours while the p27 half-life drops to between 0 and 2 hours in the presence of MEK^{EE}. In agreement with this, treatment of cells with U0126, a MEK inhibitor, increased p27 half-life. (Fig. 1D). Induction of WT p27 for 24 hours with 2 μM muristerone A resulted in an increase in p27 levels. Muristerone A was removed form the culture media (t=0) and the decline in p27 protein levels was monitored up to 24 hours after the removal of muristerone A. In the absence of U0126 p27 half-life was between 4-8 hours, while inhibition of MEK with U0126 prolonged p27 half-life to between 16-24 hours. Together these data point to a role for the MAP kinase pathway in p27 degradation.

We then wished to determine whether the MAP kinase pathway played a role in the nuclear export of p27. Cells were transiently transfected with MEK^{EE} and separated into nuclear and cytoplasmic fractions. Immunoblots of these lysates suggested an accumulation of p27 in the cytoplasm in the presence of MEK^{EE} (Fig. 2A). We also noticed the appearance of the 22 kDa previously reported by Ishida et al. in MEK^{EE} treated cells (7), although the significance of this remains unclear at this point. To determine whether this cytoplasmic accumulation of p27 was a result of a MAP kinase-induced increase in p27 nuclear export, we conducted nuclear export assays as previously described (5) either in the presence or absence of MEK^{EE} (Fig. 2B). These assays revealed that MEK^{EE} transfection increased p27 nuclear export, with maximum export being achieved within 5 minutes in MEK^{EE} transfected cells, while non-transfected cells reached maximum export at approximately 15 minutes. In agreement with our previous findings, p27 export is independent of cdk 2 activation (Fig. 2C). Treatment of cells with the cdk 2 inhibitor roscovitine did not prevent the accumulation of p27 in the cytoplasm and it is unlikely that the MEK^{EE}-induced phenomenon in Fig. 2B is also independent of cdk 2 activity.

It has been established that phosphorylation of p27 at S10 is an important mediator of p27 proteolysis. However, we see the opposite effect of S10 phosphorylation on p27 stability compared to that reported in NIH 3T3 fibroblasts (7). While others report a reduction in p27 stability by mutation of S10 to alanine (S10A) to prevent phosphorylation at that site, we show that S10A p27 protein is more stable in MCF-7 cells (Fig. 3A, unpublished observations). When WT or S10A p27 is induced with muristerone A, WT p27 protein levels return to those of uninduced cells (UI) faster than does S10A p27. This discrepancy between our results and those of others may highlight a difference in p27 regulation in mouse and human cells. We also show by 2-dimensional isoelectric focusing (2-D IEF) that the phosphorylation patterns of WT and S10A p27 are drastically different from each other. Only spots 2 and 6 are common, while spots 10-14 are unique to S10A p27. We know that S10A p27 is not exported to the cytoplasm (5) and it may be this difference in phosphorylation that accounts for the reduced p27 export and the alteration in S10A p27 stability. In order to determine whether the MAP kinase pathway can alter p27 phosphorylation we treated cells expressing WT or S10A p27 with U0126 and subjected the lysates to 2-D IEF (Fig. 4A and B). Surprisingly, we observed little effect of U0126 on WT p27, showing only a subtle shift in phosphopattern (Fig 4A). However, when we examined S10A p27, there was a loss of 2 phosphospots (Fig. 4B arrows) following treatment of cells expressing S10A p27 with U0126. In order to gain a clearer picture I must evaluate the phosphorylation of both WT and S10A p27 using 2 dimensional phosphopeptide analysis. I have already devloped the technique for another protein (RNF11, Fig. 4C) and am currently in the process of conducting like analyses for WT and S10A p27.

Key Research Accomplishments

1. Generation and characterization of cell lines that inducibly express S10A, T157A and T187A phosphomutant p27 proteins

2. Establishment of the MAP kinase pathway as an important regulator of p27 phosphorylation.

3. Illustrating the role of the MAP kinase pathway in regulating p27 nuclear export.

4. Establishing the importance of the phosphorylation of p27 by MAP kinase in regulating the recently elucidated, non-cyclin E/cdk 2 dependent degradation of p27 protein.

5. Submission and/or publication of 3 research papers/manuscripts.

Reportable Outcomes

1. **Connor, M.K.**, Kotchetkov, R., Cariou, S., Beniston, R.G., Resch, A., Lupetti, R., Melchior, F., Hengst L. and Joyce M. Slingerland. Nuclear export of $p27^{Kip1}$ is CRM1/Ran-mediated and involves a nuclear export signal and Ser10 phosphorylation. *Mol. Biol. Cell* **14,** 201-213, 2003. See Appendix 1.

2. Liang, J., Zubovitz, J., Petrocelli, T., Kotchetkov, R., **Connor, M.K.**, Han, K., Lee, J.-H., Ciarallo, S., Catzavelos, C., Beniston, R., Franssen, E. and J.M. Slingerland. PKB/AKT phosphorylates p27, impairs nuclear import of p27 and opposes p27-mediated G1 arrest. *Nat. Med.* **8,** 1153-1160, 2002. See appendix 1.

3. Sandhu, C., **Connor, M.K.**, Kislinger, T., Slingerland, J.M. and A. Emili. Cell cycle dependent proteome expression in breast cancer cells. Submitted to *J. Biol. Chem.* June 2, 2003.

4. Applied for Cell Biologist Assisstant Professor position at University of Toronto at Scarborough, Department of Life Sciences May 2002.

5. Applied for Human Biology Assisstant Professor position at University of Toronto at Scarborough, Department of Life Sciences May 2002.

6. Applied for Cell Biologist Assisstant Professor position at University of Toronto at Scarborough, Department of Life Sciences Nov 2002.

7. Applied for Cell Physiology Assisstant Professor position at York University, Department of Kinesiology and Health Sciences, Jan. 2003. Defeated by a vote of 3-2 by search committee.

8. Applied for Director of the Core Molecular Facility at Sunnybrook & Women's College Health Sciences Centre, April, 2003. Core facility will conduct research on many aspects of multiple cancers, including breast cancer.

Conclusions

From the data contained within this report we can see a clear role for the MAP kinase pathway in p27 degradation. It appears that phosphorylation of p27, mediated by MAP kinase, results in an accelerated nuclear export of p27 and an increase in p27 proteolysis. It is known that activation of the RAS pathway, which includes MAP kinase, can lead to a more aggressive cancer phenotype (1). It remains unclear as to whether MAP kinase phosphorylates p27 directly or whether these effects on p27 are just a secondary result of MAP kinase activation. Generation of a 2-dimensional phosphopeptide map of p27 should allow for a better determination of the nature of these MAP kinase effects. Regardless, the data at present are almost complete enough to propose a mechanism of MAP kinase effects on p27 degradation. I forsee these results being ready for submission for publication in the near future and these findings will hopefully help to forge a new pathway for therapeutic discovery.

References

1. Aktas, H., Cai, H. & Cooper, G.M. Ras links growth factor signalling to the cell cycle machinery via regulation of cyclin D1 and the cdk inhibitor $p27^{Kip1}$. *Mol.Cell.Biol.* **17**, 3850-3857 (1997).

2. Carrano, A., Eytan, E., Hershko, A. & Pagano, M. Skp2 is required for the ubiquitin-mediated degradation of the Cdk-inhibitor p27. *Nature Cell Biol.* **1**, 193-199 (1999).

3. Catzavelos, C., Bhattacharya, N., Ung, Y.C., et al. Decreased levels of the cell cycle inhibitor p27Kip1 protein: prognostic implications in primary breast cancer. *Nature Med.* **3**, 227-230 (1997).

4. Cheng M, Sexl V, Sherr CJ, Roussel MF. Assembly of cyclin D-dependent kinase and titration of p27Kip1 regulated by mitogen-activated protein kinase kinase (MEK1). *Proc. Natl. Acad. Sci. USA* **95**, 1091-1096 (1998).

5. Connor, M.K., Kotchetkov, R., Cariou, S., Beniston, R.G., Resch, A., Lupetti, R., Melchior, F., Hengst L. & Joyce M. Slingerland. Nuclear export of $p27^{Kip1}$ is CRM1/Ran-mediated and involves a nuclear export signal and Ser10 phosphorylation. *Mol. Biol. Cell* **14,** 201-213 (2003).

6. Delmas, C., Manenti, S., Boudjelal, A., Peyssonnaux, C., Eychene, A., and J.M. Darbon. The p42/p44 mitogen-activated protein kinase activation triggers p27Kip1 degradation independently of CDK2/cyclin E in NIH 3T3 cells. J. Biol. Chem. **276,** 34958-34965 (2001).

7. Ishida, N., Kitagawa, M., Hatakeyama, S. & Nakayama, K. Phosphorylation at Serine 10, a major phosphorylation site of p27Kip1, increases its protein stability. *J.Biol.Chem.* **275**, 25146-25154 (2000).

8. Kawada, M., Yamagoe, S., Murakami, Y., Suzuki, K., Mizuno, S. & Uehara, Y. Induction of p27Kip1 degradation and anchorage independence by Ras through the MAP kinase signaling pathway. *Oncogene* **15**, 629-637 (1997).

9. Loda, M., Cukor, B., Tam, S.W., et al. Increased proteasome-dependent degradation of the cyclin- dependent kinase inhibitor p27 in aggressive colorectal carcinomas. *Nature Med.* **3**, 231-234 (1997).

10. Pagano, M., Tam, S.W., Theodoras, A.M., et al. Role of ubiquitin-proteasome pathway in regulating abundance of the cyclin-dependent kinase inhibitor p27. *Science* **269**, 682-685 (1995).

11. Polyak, C., Lee, M.-H., Erdjument-romage, H., et al. Cloning of p27KIP1, a cyclin-dependent kinase inhibitor and a potential mediator of extracellular antimitogenic signals. *Cell* **78**, 59-66 (1994).

12. Sherr, C.J., & Roberts, J.M. CDK inhibitors: positive and negative regulators of G1-phase progression. Genes Dev. **13,** 1501-1512 (1999).

13. Slingerland, J. & Pagano, M. Regulation of the Cdk inhibitor p27 and its deregulation in cancer. *J. Cell Physiol.* **183**, 10-17 (2000).

14. Takuwa, N. & Takuwa, Y. Ras activity late in G1 phase required for p27kip1 downregulation, passage through the restriction point, and entry into S phase in growth factor-stimulated NIH 3T3 fibroblasts. *Mol.Cell. Biol.* **17**, 5348-5358 (1997).

15. Tsihlias, J., Kapusta, L. & Slingerland, J. The prognostic significance of altered cyclin-dependent kinase inhibitors in human cancer. *Annu.Rev.Med.* **50**, 401-423 (1999).

16. Tsvetkov, L.M., Yeh, K.H., Lee, S.J., Sun, H. & Zhang, H. p27(Kip1) ubiquitination and degradation is regulated by the SCFSkp2 complex through phosphorylated thr187 in p27. *Curr.Biol.* **9**, 661-664 (1999).

17. Vlach, J., Hennecke, S. & Amati, B. Phosphorylation-dependent degradation of the cyclin-dependent kinase inhibitor $p27^{Kip1}$. *EMBO J.* **16**, 5334-5344 (1997).

19. Yang HY, Zhou BP, Hung MC, Lee MH. Oncogenic signals of HER-2/neu in regulating the stability of the cyclin-dependent kinase inhibitor p27. *J. Biol. Chem.* **275,** 24735-24739, (2000).

Appendices

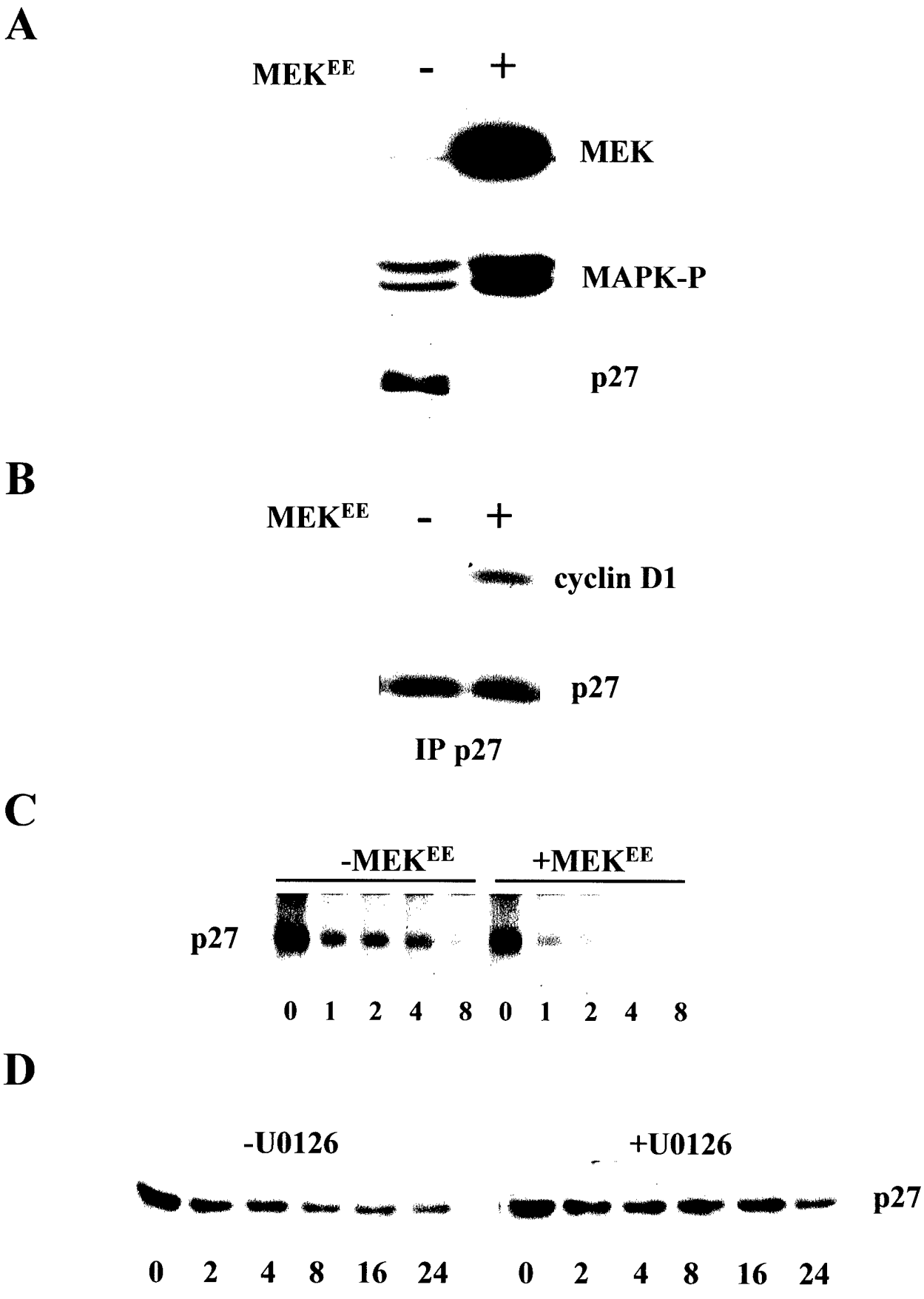
A
MEK^EE - +
MEK
MAPK-P
p27
B
MEK^EE - +
cyclin D1
p27
IP p27
C
-MEK^EE
+MEK^EE
p27
0 1 2 4 8 0 1 2 4 8
D
-U0126
+U0126
p27
0 2 4 8 16 24 0 2 4 8 16 24

Figure 1

A

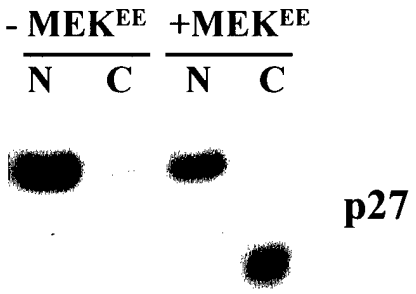
- MEK^EE
+MEK^EE
N C N C
p27

B

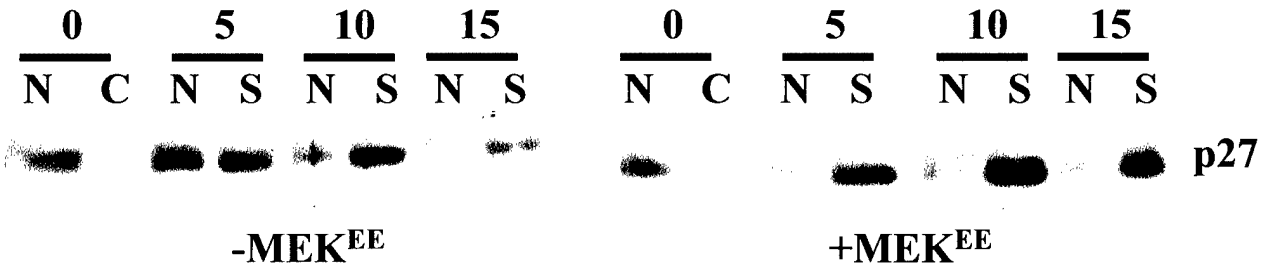
0 5 10 15 0 5 10 15
N C N S N S N S N C N S N S N S
p27
-MEK^EE
+MEK^EE

C

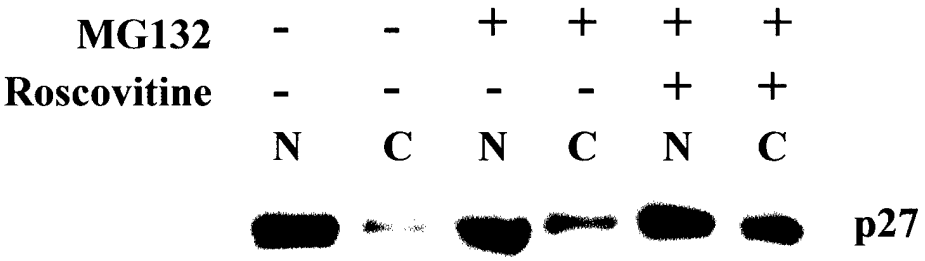
MG132 - - + + + +
Roscovitine - - - - + +
N C N C N C
p27

Figure 2

A

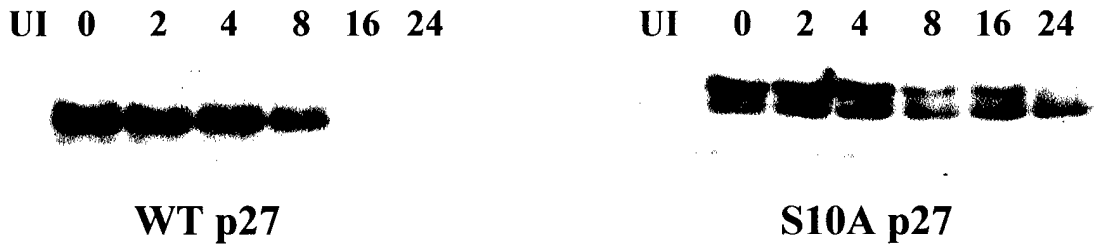
UI 0 2 4 8 16 24
UI 0 2 4 8 16 24
WT p27
S10A p27

B

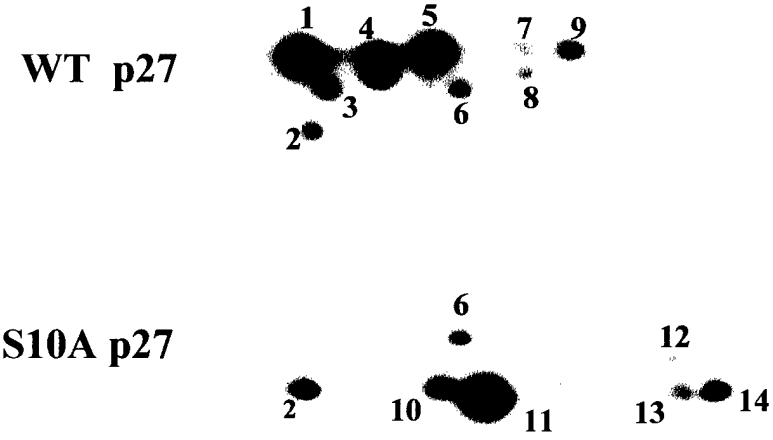
WT p27
1
4
5
7
9
3
6
8
2
S10A p27
6
12
2
10
11
13
14

Figure 3

A


WT p27 - U0126
WT p27+ U0126

B

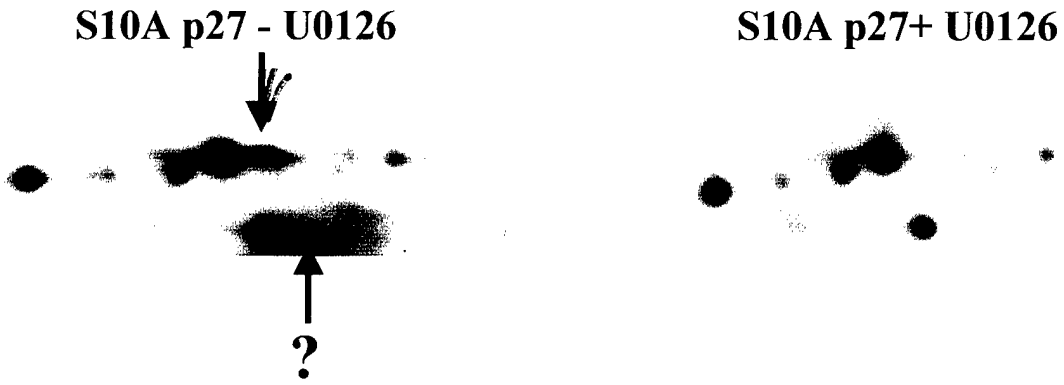
S10A p27 - U0126
S10A p27+ U0126
?

C

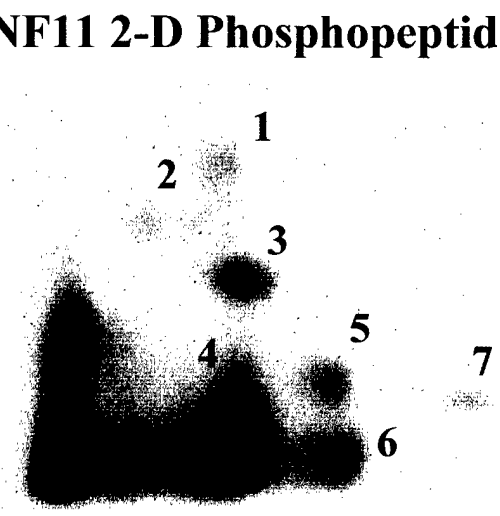
RNF11 2-D Phosphopeptide Map
1
2
3
4
5
6
7

Figure 4

Figure Legends

Fig.1. (A) MCF-7 cells were transiently transfected with a constitutively active MEK^{EE} expression vector (+). Lysates were immunoblotted for MEK, phosphorylated MAP kinase (MAPK-P) and p27. (B) p27 was immunoprecipitated from the lysates in A and probed for associated cyclin D1. (C) Cells were labeled with ^{35}S-methionine and p27 was immunopreciptated at various times following chase with 100X excess of cold methionine. (D) WT p27 was induced by treatment of cells with 2 μM muristerone A (murA) for 24 hrs (0). Cells were washed and cells were harvested at various times following this wash. Lysates were immunoblotted for p27.

Fig.2. (A) Cells were transfected with MEKEE and separated into nuclear (N) and cytoplasmic (C) fractions. Lysates were immunoblotted for p27. (B) Digitonin-permeabilized nuclei from cells with (+) or without (-) transfected MEK^{EE} were incubated with cytosolic proteins from 5-15 mins. Reactions were centrifuged and nuclear (N) and supernatant (S) fractions were probed with p27 antibodies. Nuclear export was indicated by movement from p27 from N to S fractions. (C) Asynchronously growing MCF-7 cells were separated into N and C in the presence or absence of the proteasome inhibitor MG132 and/or the cdk 2 inhibitor roscovitine.

Fig.3. (A) WT or S10A p27 was induced in cells for 24 hrs (0) by treatment with (murA). The murA was removed and lysates collected for up to 24 hrs. Lysates were immunoblotted for p27. (B) p27 proteins from A were resolved into distinct phosphoforms by 2-dimensional isoelectric focusing (2-D IEF) and probed for p27.

Fig.4. (A) WT p27 was induced witrh murA in the presence (+) or absence (-) of the MEK inhibitor U0126 and subjected to 2-D IEF. (B) S10A p27 was induced with murA in the presence (+) or absence (-) of the MEK inhibitor U0126 and subjected to 2-D IEF. (C) WM239 malignant melanoma cells were transfected with FLAG-tagged RNF11. ^{32}P labeled FLAG immunoprcipitates were digested with trypsin and subjected to separation by charge (x-direction) and thin-layer chromatography (y-direction).

Molecular Biology of the Cell
Vol. 14, 201–213, January 2003

CRM1/Ran-Mediated Nuclear Export of p27^{Kip1} Involves a Nuclear Export Signal and Links p27 Export and Proteolysis

Michael K. Connor,* Rouslan Kotchetkov,* Sandrine Cariou,* Ansgar Resch,† Rafaella Lupetti,† Richard G. Beniston,* Frauke Melchior,† Ludger Hengst,†‡ and Joyce M. Slingerland*§‡

Molecular and Cell Biology, Sunnybrook & Women's College Health Science Centre, 2075 Bayview Ave, Toronto, Ontario, Canada, M4N 3M5; and Max Planck Institute for Biochemistry, Martinsried, 82152, Germany

Submitted June 4, 2002; Revised September 27, 2002; Accepted October 3, 2002
Monitoring Editor: Mark J. Solomon

We show that p27 localization is cell cycle regulated and we suggest that active CRM1/RanGTP-mediated nuclear export of p27 may be linked to cytoplasmic p27 proteolysis in early G1. p27 is nuclear in G0 and early G1 and appears transiently in the cytoplasm at the G1/S transition. Association of p27 with the exportin CRM1 was minimal in G0 and increased markedly during G1-to-S phase progression. Proteasome inhibition in mid-G1 did not impair nuclear import of p27, but led to accumulation of p27 in the cytoplasm, suggesting that export precedes degradation for at least part of the cellular p27 pool. p27-CRM1 binding and nuclear export were inhibited by S10A mutation but not by T187A mutation. A putative nuclear export sequence in p27 is identified whose mutation reduced p27-CRM1 interaction, nuclear export, and p27 degradation. Leptomycin B (LMB) did not inhibit p27-CRM1 binding, nor did it prevent p27 export in vitro or in heterokaryon assays. Prebinding of CRM1 to the HIV-1 Rev nuclear export sequence did not inhibit p27-CRM1 interaction, suggesting that p27 binds CRM1 at a non-LMB-sensitive motif. LMB increased total cellular p27 and may do so indirectly, through effects on other p27 regulatory proteins. These data suggest a model in which p27 undergoes active, CRM1-dependent nuclear export and cytoplasmic degradation in early G1. This would permit the incremental activation of cyclin E-Cdk2 leading to cyclin E-Cdk2-mediated T187 phosphorylation and p27 proteolysis in late G1 and S phase.

INTRODUCTION

The Cdk inhibitor p27 is an important regulator of G1 progression. It is highly expressed in G0, where it binds tightly and inhibits cyclin E-Cdk 2 (Hengst *et al.*, 1994; Polyak *et al.*, 1994; Slingerland *et al.*, 1994). In mid-G1, p27 also plays a role in the assembly and nuclear import of D-type cyclin-Cdk complexes (LaBaer *et al.*, 1997; Cheng *et al.*, 1999). p27 levels are regulated by translational controls and by proteolysis, and decrease as cells progress from G1 to S phase (Hengst and Reed, 1996; Millard *et al.*, 1997; Slingerland and Pagano, 2000). The ubiquitin-dependent proteolysis of p27 (Pagano *et al.*, 1995) is regulated by its phosphorylation at threonine 187 (T187) by cyclin E-Cdk 2 in late G1 and S phase (Sheaff *et al.*, 1997; Vlach *et al.*, 1997; Montagnoli *et al.*, 1999). T187 phosphorylation allows recognition of p27 by its SCF-type E3 ligase, comprised of Skp1, Cul1, and the *F*-box protein, Skp2 and Roc1 and the Cks1 cofactor (Carrano *et al.*, 1999; Ohta *et al.*, 1999; Sutterluty *et al.*, 1999; Tsvetkov *et al.*, 1999; Ganoth *et al.*, 2001; Spruck *et al.*, 2001). Recent evidence suggests that p27 proteolysis is regulated by at least two distinct mechanisms, with mitogenic signaling conditioning p27 for degradation in early G1 in a manner independent of T187 phosphorylation (Hara *et al.*, 2001; Malek *et al.*, 2001), whereas Skp2-dependent cyclin E-Cdk 2-mediated degradation occurs in S phase after T187 phosphorylation (Malek *et al.*, 2001).

Article published online ahead of print. Mol. Biol. Cell 10.1091/mbc.E02–06–0319. Article and publication date are at www.molbiolcell.org/cgi/doi/10.1091/mbc.E02–06–0319.

‡ Corresponding authors. E-mail address: jslingerland@med.miami.edu or hengst@biochem.mpg.de
§ Present address: University of Miami Sylvester Comprehensive Cancer Center, Division of Hematology Oncology, Miami Florida, 33133

Although p27 is detected in the nuclei of most normal quiescent cells (Slingerland and Pagano, 2000), the relationship between its intracellular localization and proteolysis has afforded some controversy. Efficient degradation of mammalian p27 and of its *Xenopus* homolog, Xic1, requires nuclear import to allow its phosphorylation by cyclin E-Cdk2 (Guan *et al.*, 2000; Swanson *et al.*, 2000). Interaction of p27 with the nuclear pore protein, Nup50/NPAP60 (Guan *et al.*, 2000; Muller *et al.*, 2000), may play a role in p27 import. A nuclear localization signal has been identified and import may also involve the binding of p27 by other import mediators (Reynisdottir and Massague, 1997; Zeng *et al.*, 2000). Nup50 antibodies have been shown to block nuclear export but not import (Guan *et al.*, 2000), thus a potential role for p27-Nup50 interaction in p27 export cannot be excluded (Smitherman *et al.*, 2000). p27 can interact with the Jun activation domain-binding protein 1 ($p38^{Jab1}$). Cotransfection of p27 together with Jab1 led to accelerated proteolysis of p27. The observation that the cytotoxin leptomycin B (LMB) inhibited Jab1-mediated p27 proteolysis suggested that CRM1-dependent nuclear export mechanisms influence p27 degradation (Tomoda *et al.*, 1999) and provided a potential link between p27 turnover and nuclear export. In contrast, the *Xenopus* homolog of p27, Xic1, is ubiquitinated in the nucleus and its proteolysis is not impaired by LMB (Swanson *et al.*, 2000).

The nuclear pore has an estimated mass of ≈125 MDa and controls nucleocytoplasmic protein exchange. Although the pore diameter permits molecules of up to 50 kDa to diffuse freely across the nuclear envelope, the localization of many small proteins is actively regulated (Mattaj and Engimeier, 1998; Gorlich and Kutay, 1999). Proteins whose function is spatially and temporally regulated, such as cyclin D1 (Alt *et al.*, 2001), cyclin B1 (Pines and Hunter, 1991, 1994; Jin *et al.*, 1998; Yang *et al.*, 1998), IκB (Huang *et al.*, 2000), and mitogen-activated protein kinase (MAPK; Adachi *et al.*, 2000), are actively transported between the nucleus and cytoplasm. This process involves a number of nucleocytoplasmic shuttling proteins. Two proteins, CRM1/exportin 1 (Fukuda *et al.*, 1997; Fornerod *et al.*, 1997; Stade *et al.*, 1997) and the small *ras* family GTPase, Ran (Melchior *et al.*, 1993; Moore and Blobel, 1993), both play prominent roles in the regulation of nuclear protein export. Ran is abundant and exists in GDP- or GTP-bound forms depending on its cellular location (Melchior and Gerace, 1998; Macara, 1999; Azuma and Dasso, 2000; Sacer and Dasso, 2000). Cytoplasmic RanGDP plays a key role in nuclear import. In the nucleus, RanGDP is converted to RanGTP by the guanine nucleotide exchange factor RCC1, and becomes competent to bind export cargo before shuttling back to the cytoplasm (Nigg, 1997; Mattaj and Engimeier, 1998; Gorlich and Kutay, 1999). The exportin protein, CRM1, binds export cargo proteins and RanGTP in the nucleus to form an export complex that is subsequently translocated to the cytoplasm (Fornerod *et al.*, 1997; Stade *et al.*, 1997; Kehlenbach *et al.*, 1998). At the cytoplasmic face, the complex is dissociated by RanGAP, in combination with either RanBP1 or RanBP2 (Nigg, 1997; Mattaj and Engimeier, 1998; Gorlich and Kutay, 1999).

In the present study, we demonstrate that nuclear export of the Cdk inhibitor, p27, is actively regulated by CRM1/RanGTP binding. Nuclear export of p27 is time, temperature, and energy dependent. Although p27 binding to CRM1 is cell cycle regulated, it is LMB insensitive and LMB has no apparent effect on CRM1-mediated p27 nuclear export either in vitro or in vivo. A putative nuclear export sequence (NES) in p27 is identified. Mutation of this NES reduced nuclear export, impaired p27-CRM1 interactions, and increased p27 stability.

MATERIALS AND METHODS

Cell Culture

MCF-7 cells were grown in improved modified Eagle's medium (IMEM) supplemented with 5% (vol/vol) fetal bovine serum (FBS). Cells were synchronized in G0 by estradiol depletion as described by Cariou *et al.* (2000). Cells were released from quiescence by the addition of 10^{-8} M 17β-estradiol (Sigma, St. Louis, MO).

Plasmids and Transfections

A vector encoding wild-type p27 fused to an enhanced yellow-green variant of the Aequorea victoria green fluorescent protein (YFPp27 WT) was prepared by insertion of the full-length wild-type human p27 cDNA sequence into the pEYFP-C1 vector (Clontech, Palo Alto, CA). Double L41A/L45A mutations were introduced into the YFPp27 WT vectors using a Quickchange site-directed mutagenesis kit (Stratagene, La Jolla, CA) to generate the YFPp27NES vector. All p27 cDNA constructs were sequenced fully to ensure the absence of cloning artifacts. Asynchronous MCF-7 cells were transfected with the different YFPp27 vectors (10 μg) using lipofectamine PLUS (GIBCO, Grand Island, NY) and were then estradiol deprived for 48 h. Assays of YFPp27 nuclear export and binding to CRM1 were carried out at 48 h posttransfection. Equal transfection efficiency was verified by direct visualization of p27 by fluorescence microscopy. For the heterokaryon assays, we used a green fluorescence protein tagged p53 construct kindly provided by G. Wahl (Stommel *et al.*, 1999).

Indirect Immunofluorescence of p27 and BrdU

MCF-7 cells were grown on glass slides, arrested in G0 by estradiol depletion (48 h), and then induced to reenter the cell cycle by the addition of 10^{-8} M 17β-estradiol. Cells were also labeled with 5-bromo-2-deoxy uridine (BrdU) to monitor the timing of S phase entrance. In G0 and at intervals after estradiol addition, cells were fixed in 4% paraformaldehyde and 0.2% Triton X-100, blocked in 3% H_2O_2 and 10% goat serum, and then incubated with a mouse mAb for p27 (BD Transduction Laboratories, Lexington, KY) and a rabbit polyclonal anti-BrdU antibody (CalTag Laboratories, Burlingame, CA). Fluorescein (FITC)-conjugated anti-mouse and Texas red-conjugated anti-rabbit secondary antibodies allowed visualization of p27 protein and BrdU incorporation, respectively. Cells were visualized by confocal fluorescence microscopy and photographed.

Detection of p27-CRM1 Complexes in Cell Lysates

At indicated times after G0 release, p27 was immunoprecipitated from 1 mg of cellular lysate using the C-19 (Santa Cruz Biotechnology, Santa Cruz, CA). Complexes were resolved and associated CRM1 was detected by immunoblotting with polyclonal CRM1 antibodies (kindly provided by R. Kehlenbach and L. Gerace or by M. Fornerod; Fornerod *et al.*, 1997; Kehlenbach *et al.*, 1998). p27 was detected in CRM1 immunoprecipitates from 1 mg of cell lysate using the Gerace laboratory anti-CRM1 antibody for immunoprecipitation.

Detection of p27-Cyclin E1-Cdk2 Complexes

To test the effect of NES mutation on the association of p27 with cyclin E1-cdk2, cells were transfected with either YFPp27WT or

YFPp27NES and cyclin E1 or YFP proteins immunoprecipitated. Complexes were resolved by SDS-PAGE and immunoblotted to detect associated proteins (cyclin E1 or p27).

Subcellular Fractionation and In Vitro Nuclear Export

Cells in G0 and early G1 were harvested and resuspended in 300 μl of an isotonic transport buffer (20 mM HEPES, pH 7.3, 110 mM KAcetate, 5 mM NaAcetate, 2 mM MgAcetate, 1 mM EGTA, and 2 mM dithiothreitol) containing protease inhibitors, 1 mM $NaVO_3$, and 50 mM NaF. Digitonin (20–30 μg/ml final concentration) was added until 90%–95% of the cells exhibited trypan blue staining. Cells were then centrifuged and the supernatant (cytoplasmic fraction) was recovered. The pellet (nuclear fraction) was washed and resuspended in 300 μl of transport buffer. The intact nuclei were then used for nuclear export assays or for immunoblotting. To assay nuclear export of p27, digitonin-permeabilized cells were incubated with fractionated cytosolic protein (75 μg), an ATP regenerating system (5 mM ATP, 5 mM creatine phosphate, and 20 U/ml creatine phosphokinase), and 2 mM GTP at room temperature for up to 30 min (Adam *et al.*, 1992). Nuclear export was stopped by centrifugation, and the supernatant was removed. p27 was immunoprecipitated from both nuclear and supernatant fractions, resolved by SDS-PAGE, and nuclear and exported p27 was detected by immunoblotting. For controls, export assays were conducted at 4°C and in the absence of cytosolic proteins, an ATP regenerating system, or both.

For detection of nuclear p27 export using indirect immunofluorescence, cells were grown on glass slides and permeabilized by incubation with 25 μg/ml digitonin for 3 min at 4°C. The cells were washed and incubated with cytosolic proteins (2.5 mg/ml) and an ATP regenerating system (as above) at room temperature for 10, 20, and 30 min. Nuclear p27 was detected by indirect immunofluorescence and fluorescence intensity quantified using laser scanning software (LSM 510; Carl Zeiss, Jena, Germany) and confocal microscopy.

To assay the expression and nuclear export of green-yellow fluorescent-tagged p27, MCF-7 cells were grown on glass slides and were transfected with wild-type or NES YFPp27 vectors. Export of p27 from digitonin-permeabilized cells was as above. Nuclear export of p27 was determined by measuring the decline in nuclear YFP fluorescence by direct photomicroscopy using a digital camera, and fluorescence intensity was quantified using Laser Scanning Software (LSM 510; Carl Zeiss).

Heterokaryon Assay

Nucleocytoplasmic shuttling of YFP-p27 and GFP-p53 was detected in HeLa/NIH 3T3 cell heterokaryons. Hela cells were grown on glass coverslips in Dulbecco's MEM (DMEM) containing 10% fetal calf serum and was transfected using Superfect reagent (Qiagen, Valencia, CA) according to the manufacturer's instructions. Cells were washed four times with DMEM medium 12 h after transfection, and NIH 3T3 cells were seeded. Cells were treated with cycloheximide (75 μg/ml) for 30 min before fusion. Cell fusion was induced by the addition of 50% (wt/vol) polyethylenglycol in DMEM for 2 min in the presence of 50 μg/ml cycloheximide. After washing four times with PBS, cells were further incubated in DMEM containing 50 μg/ml cycloheximide for 2 h to allow shuttling. To the indicated samples, LMB (final concentration 50 ng/ml) was added 2 h before cell fusion.

After washing with PBS, cells were fixed with 3.7% formaldehyde in PBS (5 min at 20°C, 10 min at 4°C). Cells were permeabilized by treatment with 0.1% Triton X in PBS (4°C) for 5 min. After washing in PBS, cells were incubated with PBS supplemented with 2% bovine serum albumin (BSA) at room temperature for 10 min. Actin was stained with 100 μl of Texas-red phalloidin (Sigma) diluted 1:2000 in PBS/2% BSA. After washing with PBS, DNA was stained with 1% Hoechst 33258 (Molecular Probes, Eugene, OR) diluted 1:2000 in PBS. Coverslips were then washed and mounted on glass slides.

p27 Nuclear Import

Quiescent MCF-7 cells were digitonin permeabilized and incubated with 4 μg/μl (final concentration) cytosolic proteins and an ATP-regenerating system at room temperature. His-tagged p27 was added, and the reactions incubated for 60 min. Reactions were stopped by centrifugation and were separated into nuclear and supernatant fractions. Where indicated, nuclei were preincubated with LMB (50 ng/ml), *N*-acetyl-leu-leu-norleucinal (LLnL; 2.5 μM), or wheat germ agglutinin (WGA; 20 μg/ml).

Recombinant Protein Assays

p27 was immunoprecipitated from 1 mg of cell lysate recovered 6 h after estradiol stimulation of quiescent MCF-7 cells. After 5 min incubation at 95°C to denature any endogenous p27-associated proteins, the supernatant containing heat-stable p27 was incubated with recombinant CRM1 in the presence or absence of GTP-loaded Ran or GDP-loaded Ran for 20 min at 4°C (Askjaer *et al.*, 1999). p27 was immunoprecipitated and the associated proteins were separated by SDS-PAGE. To assess if p27-CRM1/Ran complexes could be dissociated in vitro, they were incubated with recombinant RanGAP and RanBP1 for 30 min at 30°C. p27 immune complexes were then centrifuged, and dissociation of CRM1 or Ran into the supernatant was assayed by immunoblotting both fractions. Similar experiments were conducted using cells transfected with the wild-type and mutant YFPp27 constructs.

Similar experiments were carried out entirely with recombinant proteins. Recombinant His-tagged p27 prepared in *Escherichia coli* or baculovirus-produced cyclin D1 proteins were mixed with recombinant CRM1 for 60 min at 4°C with or without pretreatment of CRM1 with LMB 100 ng/ml for 30 min. p27 or cyclin D1 was immunoprecipitated, complexes were resolved, and associated CRM1 was detected by immunoblotting.

To test the effect of HIV-1 Rev on p27-CRM1 and cyclin D1-CRM1 complexes, the HIV-1 Rev NES peptide, NH2-CLPPELERLTL-COOH (Kudo *et al.*, 1998), was synthesized and purified over reverse-phase high-performance liquid chromatography (HPLC) on a C8 column and was verified by mass spectrophotometry. A molar excess of peptide was preincubated with recombinant CRM1 for 30 min at 4°C before the addition of RanGTP and p27 or cyclin D1 proteins for an additional 60 min. p27 or cyclin D1 immune complexes were then assayed for associated CRM1 by IP blots.

Microinjection of Nuclei and Assays of Nuclear Export of p27-NES-Peptide Coupled to BSA

Export ligand preparation followed published procedures (Melchior, 1998). In brief, fatty acid-free BSA (Boehringer Mannheim, Indianapolis, IN) was conjugated with FITC isomer I (Molecular Probes) and was purified via gel filtration. Peptides containing the putative p27 nuclear export sequence (CRNLFGPVDHEELTRDLE) were coupled to FITC-BSA via their N-terminal cysteine using the cross-linker, Sulfo-SMCC (Pierce, Rockford, IL). Microinjection of FITC-BSA-NES and FITC-BSA (0.1 mg/ml) into nuclei of adherent HeLa cells was performed with an Eppendorf Femtojet. Cells were kept at 37°C, and photomicrographs were taken at different times after injection using an inverted fluorescence microscope (IX70; Olympus, Melville, NY) and a back-illuminated charged-coupled device camera (Princeton Instruments, Trenton, NJ).

RESULTS

p27 Localization Is Cell Cycle Regulated

p27 localization was assayed at intervals across the cell cycle in synchronized MCF-7 cells (Cariou *et al.*, 2000). p27 levels

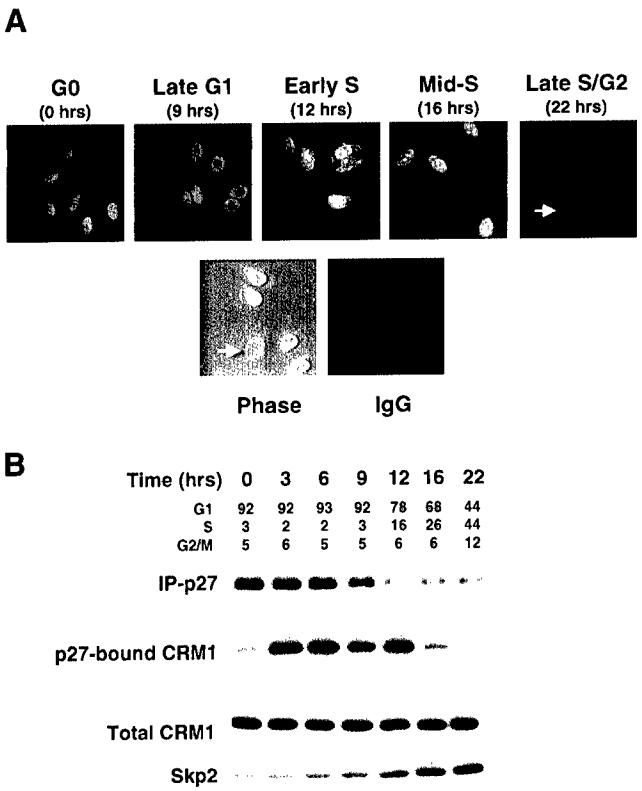

Figure 1. p27 localization and CRM1-binding are cell cycle dependent. Cell cycle entry of quiescent MCF-7 cells was induced by the addition of 17β-estradiol at time 0. Cells were assayed at intervals thereafter for p27 localization (A) or for protein assays and cell cycle profiles (B). (A) MCF-7 cells grown on glass slides were arrested in G0 by estrogen depletion. After stimulation with estradiol, p27 levels (green) and BrdU uptake (red) were visualized by confocal fluorescence microscopy at intervals across the cell cycle. Cells negative for both p27 and BrdU staining were evident in the late S phase/G2 population (white arrow). These unstained cells are apparent on phase contrast imaging of the same field. Control cells stained with nonspecific control IgG followed by FITC and Texas Red conjugated antibodies are shown (IgG). (B) Transient binding of p27 to CRM1 occurs early in G1. p27 was immunoprecipitated at intervals across the cell cycle, p27 complexes were resolved, and immunoblots were probed for p27 and CRM1. The same cell lysates were immunoblotted for CRM1 and Skp2. The cell cycle profile at each time point was assayed by dual propidium iodide/BrdU labeling and flow cytometry.

and BrdU uptake were monitored by indirect immunofluorescence labeling and confocal microscopy. Quiescent MCF-7 cells exhibited strong nuclear p27 expression (Figure 1A, G0). Nuclear p27 intensity fell progressively as cells moved through G1. At 9 h after estradiol addition, late G1 cells showed predominantly nuclear p27, with some cells showing both cytoplasmic and nuclear p27 localization. Twelve hours after G0 release, at a time when p27 is known to undergo rapid proteolysis (Malek *et al.*, 2001), early S phase cells exhibiting both nuclear and cytosolic p27 were consistently detected, suggesting either delayed import or that nuclear p27 export exceeds import (Figure 1A, early S). Because new p27 synthesis is dramatically decreased within hours of G0 exit (Hengst and Reed, 1996; Millard *et al.*, 1997; S. Cariou and J.M. Slingerland, unpublished MCF-7 data), the latter may be more likely. During S phase (t = 16–22 h), p27 became progressively undetectable in cells staining positive for BrdU uptake. In late S/early G2 cell populations, some cells were negative for both p27 staining and BrdU uptake (Figure 1A, see dual negative cell indicated by white arrow). Flow cytometry of cells at each time point in Figure 1A is shown in Figure 1B.

p27-Bound CRM1 Increases during G1 Progression

A major mechanism of nuclear export involves binding of the export cargo protein to the exportin CRM1. Cells were synchronized in parallel with those assayed in Figure 1A above. Immunoprecipitation of cellular p27 at intervals between G0 and S phase revealed an association between p27 and CRM1 that increased during G1 as p27 levels decreased (Figure 1B). p27 was also found to interact with Ran in early G1 in coimmunoprecipitation experiments (M. Connor and J. Slingerland, unpublished results). CRM1 levels were constant across the cell cycle. Given the reduction in p27 in the 6- to 12-h time points, the increase in p27-bound CRM1 is dramatic as cells move through G1 toward late G1/S. The increase in levels of p27-bound CRM1 is temporally associated with the activation of p27 proteolysis demonstrated earlier as cells move from G0 to G1 and S phase (Pagano *et al.*, 1995; Hengst and Reed, 1996; Malek *et al.*, 2001). The onset of this transient binding of p27 to CRM1 occurs before the increase in Skp2 protein levels observed 12 h after the addition of estradiol (Figure 1B). In addition, the onset of p27-CRM1 binding occurs before activation of cyclin E-Cdk2 in this cell line (Cariou *et al.*, 2000).

Nuclear Export of p27 Is Actively Regulated

The cell cycle-dependent changes in localization of endogenous p27 led us to investigate how nuclear export of p27 is regulated. To assay nuclear export of p27, MCF-7 cells were grown on glass slides, synchronized in quiescence, and released into the cell cycle. In mid-G1 (6 h after release from quiescence), cells were treated with digitonin at concentrations that selectively permeabilize the cytoplasmic membrane and leave the nuclear membrane intact. Nuclear export of cellular p27 was detected by indirect immunofluorescence at intervals after the addition of ATP, an ATP-regenerating system, and cytosolic proteins (Figure 2A). A second method was used to demonstrate and quantitate p27 export. Nuclei were separated from cytosolic proteins by digitonin-permeabilization of cells in mid-G1. In vitro export of nuclear p27 was assayed by immunoblotting of nuclear p27 and p27 exported into the supernatant over time (Figure 2B). Passive diffusion of p27 from the nuclei was not observed in the absence of ATP or at 4°C in either of these assays, indicating that p27 export is actively regulated (Figure 2, A and B). In vitro export of p27 from G0 nuclei proceeded at a rate 50% slower than that from mid-G1 nuclei (Figure 2B). Thus, as cells progress from G0 into mid-G1, p27 or other cofactors may be modified to facilitate nuclear export. The rate of p27 export assayed by densitometric analysis of p27 blots in Figure 2B was similar to that measured by the decay in nuclear p27 fluorescence quantitated

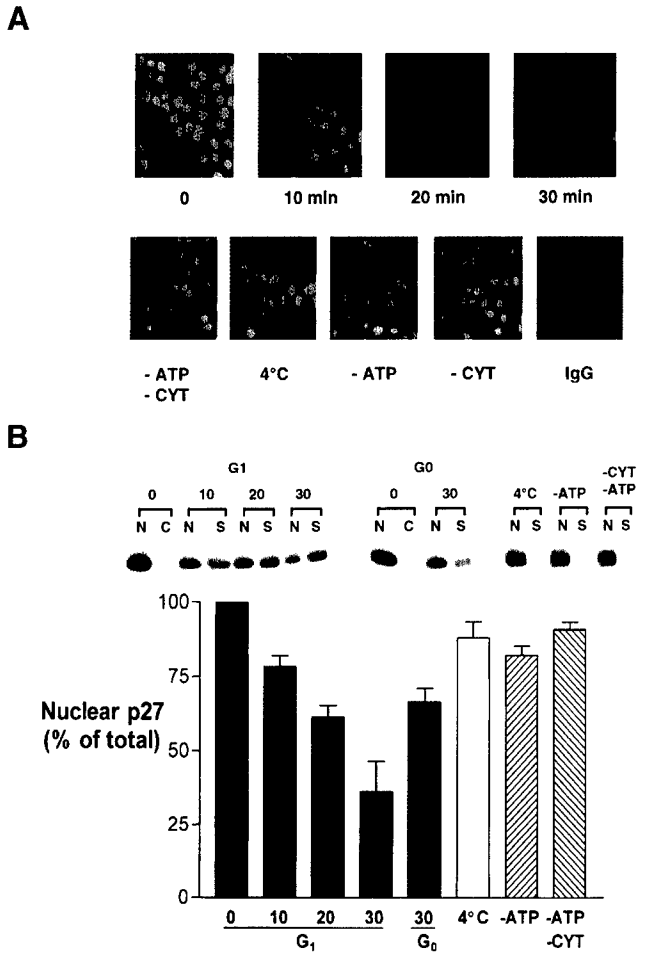

Figure 2. Active nuclear export of p27. (A) Cells were grown on glass slides and synchronized as in Figure 1. Six hours after induction of cell cycle entry by 17β-estradiol addition, cells were digitonin permeabilized and subjected to export assays, fixed, and nuclear p27 visualized by indirect immunofluorescence. (B) Cells were recovered in either mid-G1 or G0 and nuclear export of p27 after digitonin permeabilization assayed as described in "Materials and Methods." At indicated times, reactions were stopped by centrifugation and p27 was assayed in nuclei (N) and supernatant (S) fractions. p27 export was minimal after 30 min in the absence of ATP (-ATP), cytosol (-CYT), or both (-ATP/–CYT).

by confocal microscopy using laser scanning software (Carl Zeiss) in Figure 2A.

p27 Interacts with CRM1 In Vitro

When CRM1 binds to export cargo in association with nuclear RanGTP, cytoplasmic dissociation of the complex is stimulated by GTP hydrolysis. To test the specificity of p27-CRM1 interactions, formation of CRM1-Ran-p27 complexes was assayed in vitro. p27 was immunoprecipitated from mid-G1 cells, boiled to dissociate heat labile proteins, and was then incubated with recombinant CRM1 and either GTP-loaded Ran (Figure 3A, lane 1) or GDP-loaded Ran (Figure 3A, lane 2). p27-CRM1-Ran complexes were readily

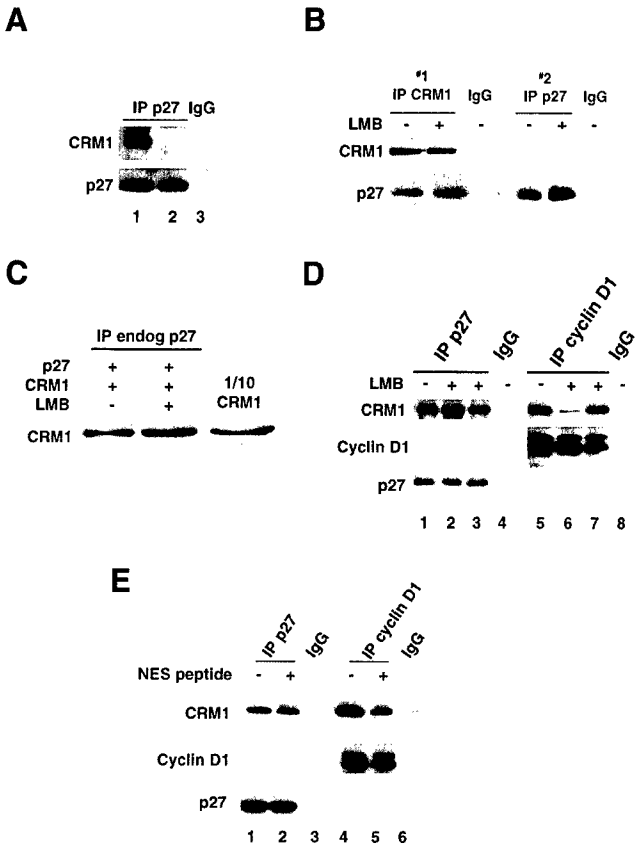

Figure 3. p27 binds CRM1 in vitro and LMB does not impair p27-CRM1 binding. (A) p27 was immunoprecipitated from cells in early G1 and incubated at 95°C for 5 min to denature heat labile-associated proteins. The supernatant containing p27 was then incubated with recombinant CRM1 together with either GTP-loaded Ran (lane 1) or GDP-loaded Ran (lane 2) for 30 min at 4°C followed by immunoprecipitation of p27. p27 antibody-bound protein A Sepharose beads did not show any nonspecific interaction with recombinant Ran or CRM1 (lane 3). (B) CRM1 was first immunoprecipitated from cells recovered in midG1 with or without prior treatment with LMB (IP #1). The supernatant was recovered and p27 was then immunoprecipitated from the CRM1-depleted lysates (IP #2). CRM1- and p27-bound proteins were immunoblotted for CRM1 and p27. Antibody only controls are shown for IP #1 and #2 (IgG). (C) The effect of LMB on binding of recombinant CRM1 to cellular p27 was assayed as in A. Equal amounts of heat stable p27 recovered from midG1 cells were reacted with recombinant RanGTP and CRM1 without (lane 1) or with (lane 2) pretreatment of the CRM1 with LMB. p27 was then immunoprecipitated and complexes were resolved and blotted for associated CRM1. One-tenth of the input recombinant CRM1 was loaded in the lane on the right. Equal amounts of p27 were immunoprecipitated in each lane (not shown). (D) Recombinant his-tagged p27 (lanes 1 through 3) or flag-tagged T286-phosphorylated cyclin D1 (lanes 5 through 7) were incubated with RanGTP and CRM1 either without (lanes 1 and 5) or with (lanes 2 and 6) pretreatment of the CRM1 with LMB. LMB was also added to the reaction mixture after complex formation (lanes 3 and 7). Antibody control lanes are also shown (lanes 4 and 8). (E) CRM1 binding assays were carried out as in D. CRM1 was preincubated with a peptide corresponding to the NES of the HIV-1 Rev protein (NES peptide) before the addition of p27 (lane 2) or cyclin D1 (lane 5).

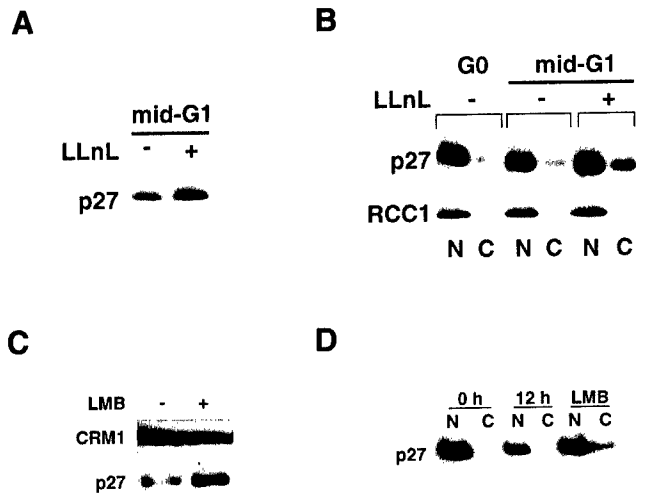

Figure 4. Both LLnL and LMB increase nuclear and cytoplasmic p27 levels. (A) Mid-G1 cells were recovered at 9 h after G0 release, with or without 6 h of LLnL treatment immediately before harvesting. Lysates were immunoblotted for p27. (B) Cells were also treated as in A above and nuclear (N) and cytoplasmic (C) fractions immunoblotted for p27. Immunoblots were probed for the nuclear protein RCC1 to verify the lack of leakage of nuclear proteins into the cytoplasm. (C and D) At 6 h after G0 release, cells were incubated either with or without LMB for an additional 6 h and whole cell lysates (C) or nuclear and cytosolic fractions (D) were immunoblotted as shown. RCC1 probing verified adequacy of fractionation (not shown).

detected in the presence of RanGTP, but were significantly reduced in the presence of RanGDP. Nonspecific binding of CRM1 or Ran to p27 antibody-bound protein A beads was not evident (Figure 3A, lane 3). p27 binding to CRM1 alone was also detected and p27-CRM1-RanGTP complexes dissociated after incubation with RanBP1 and RanGAP (M. Connor and J.M. Slingerland, unpublished results). These data support the specific association of p27, CRM1, and Ran complex formation in early G1 regulating nuclear export of p27.

LMB Increases p27 Levels But Does Not Disrupt p27-CRM1 Binding

Treatment of cells with LMB increased p27 levels (Figure 3B, right panel and Figure 4C). Densitometric analysis of repeat experiments showed that ~18% of total cellular p27 was detected in CRM1 complexes at 9 h after release from G0. However, LMB treatment did not appear to impair endogenous cellular p27-CRM1 interaction (Figure 3B). To further explore this unexpected result, we assayed p27-CRM1 binding in vitro by two different methods. Pretreatment of recombinant CRM1 with a molar excess of LMB in vitro did not impair the binding of CRM1 to heat stable p27 isolated from cells in mid-G1 (Figure 3C), nor did it impair CRM1 binding to His-tagged recombinant p27 protein (Figure 3D, lane 1 versus lane 2). In contrast, CRM1 binding to cyclin D1 was impaired by LMB. CRM1 binding to cyclin D1 was assayed using flag-tagged recombinant cyclin D1, phosphorylated at T286 in vitro with GSK-3β to promote binding to CRM1 (Alt *et al.*, 2001). Cyclin D1-bound CRM1 was substantially reduced by pretreatment of the recombinant CRM1 with LMB (Figure 3D, lane 5 versus lane 6). LMB was unable to dissociate CRM1-bound p27 or cyclin D1 when it was added to these respective complexes subsequent to mixing of the recombinant proteins (Figure 3D, lanes 3 and 7).

HIV-1 Rev NES Peptide Competes with CRM1 Binding to Cyclin D1 But Not to p27

Active nuclear export involves binding of an exportin to a NES motif on the export substrate (Mattaj and Engimeier, 1998; Gorlich and Kutay, 1999). The exportin, CRM1 binds to classical NES-containing proteins via an LMB-sensitive domain. The failure of LMB to inhibit CRM1 binding to p27 both in vivo and in vitro raised the possibility that p27 interacts with CRM1 in a novel manner. To test this, we assayed the effect of prebinding CRM1 to the classical NES motif of the HIV-1 Rev protein on the association between p27 and CRM1 and between cyclin D1 and CRM1 in vitro. CRM1 was preincubated with a 10 amino acid peptide corresponding to the HIV Rev NES (NH2-CLPPLRLTL-COOH) for 30 min before the addition of RanGTP and either p27 or cyclin D1. Preincubation of CRM1 with the HIV-1 Rev NES peptide did not reduce the amount of CRM1 that bound to p27 (Figure 3E, lane 1 versus lane 2). In contrast, the NES peptide reduced cyclin D1/CRM1 interaction (Figure 3E, lane 4 versus lane 5).

Proteasome Inhibition and LMB Increase Detectable Cytoplasmic p27

Recent reports suggest that p27 degradation is complex and may involve both T187-dependent and -independent proteolytic mechanisms (Sheaff *et al.*, 1997; Malek *et al.*, 2001; Ishida *et al.*, 2002). If even a portion of cellular p27 undergoes nuclear export before cytosolic degradation, proteasome inhibition should lead to accumulation of p27 within the cytoplasm. As shown previously (Pagano *et al.*, 1995), proteasome inhibitors increased p27 protein levels (Figure 4A). Nuclear-cytoplasmic fractionation confirmed the data in Figure 1A that in G0, p27 is almost exclusively nuclear (Figure 4B). A modest reduction of p27 was notable by 9 h after G0 release, with a minor amount of p27 in the cytoplasm. LLnL treatment in mid-G1 led to increases in both nuclear and detectable cytoplasmic p27 levels. The nuclear:cytoplasmic ratios of p27 were 9.2:1 and 4.5:1 for cells in mid-G1 in the absence or presence of LLnL, respectively. Because LLnL appears not to delay either export or import of p27 (see below, Figure 5), these data are consistent with degradation of at least part of the cellular p27 pool occurring in the cytoplasm.

To further investigate the effect of LMB on p27 levels and localization, MCF-7 cells were released from quiescence for either 12 or 6 h followed by addition of 200 ng/ml LMB for an additional 6 h and nuclear and cytoplasmic fractions were isolated. LMB treatment in mid-G1 inhibited the reduction in p27 levels that occurred in when cells progress into early S phase (Figure 4, C and D). Although LMB caused an accumulation of p27, it did not sequester p27 exclusively within the nucleus (Figure 4D). p27 levels were increased in both the nucleus and in the cytoplasm, exhibiting a pattern similar to that observed after inhibition of

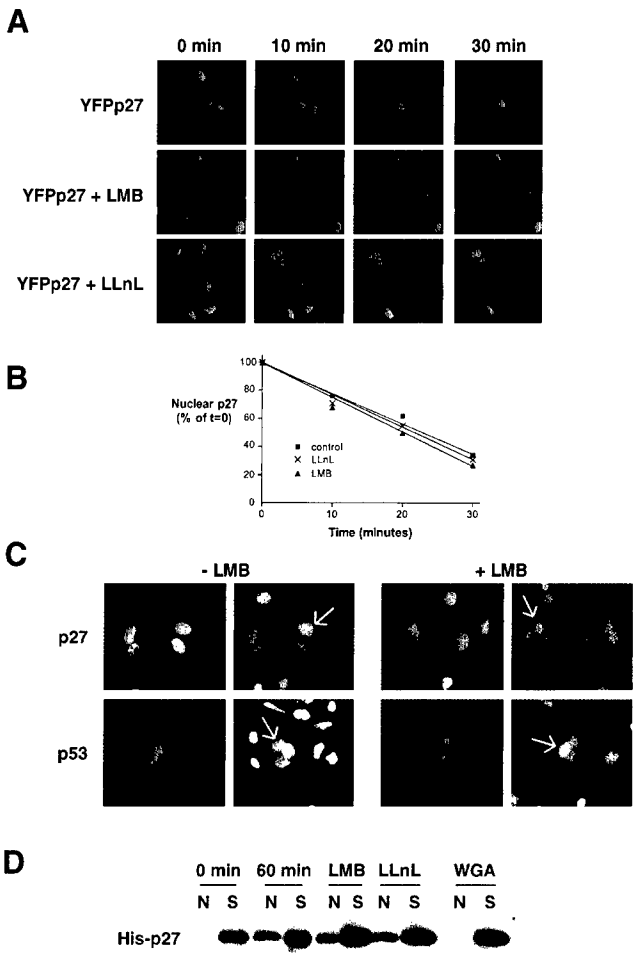

Figure 5. LMB does not prevent p27 nuclear export in vitro or in vivo. (A) MCF-7 cells were transfected with YFPp27WT and arrested in quiescence. Cells were digitonin permeabilized and incubated with 2.5 mg/ml cytosolic proteins and an ATP regenerating system. Incubations were carried out for the indicated times at room temperature. Where indicated, cells were pretreated with LMB or LLnL to assess the affects of these drugs on p27 nuclear export. (B) The decay of nuclear p27 fluorescence in A was visualized by direct fluorescence microscopy, photographed with a digital camera, quantitated using Carl Zeiss laser scanning software (LSM) 510, and graphed as a function of time. (C) Hela cells transfected with expression vectors for either YFPp27 or GFPp53 were fused to nontransfected NIH 3T3 cells (white arrow) in the presence or absence of LMB. The localization of either YFPp27 or GFPp53 (green) was visualized by fluorescence microscopy. Cells were fixed and stained for actin (red). Nuclei were visualized by staining the DNA with Hoechst 33258 (black and white panels). (D) p27 nuclear import was assessed by the addition of his-tagged p27 (His-p27) to digitonin-permeabilized cells in the presence of cytosolic proteins (4 μg/μl) and an ATP regenerating system. Reactions were centrifuged and nuclear (N) and supernatant (S) fractions were immunoblotted for p27. Nuclei preincubated with 200 μg/ml WGA showed no import of p27.

proteolysis by LLnL (Figure 4B). Immunoblotting for RCC1 showed no escape of nuclear protein into the cytoplasmic fractions (M. Connor and J.M. Slingerland, unpublished results).

LLnL and LMB Do Not Prevent Nuclear Export of p27 In Vitro or In Vivo

In the context of Jab-1 overexpression, LMB has been shown to inhibit the cytoplasmic accumulation of p27 and its proteolysis (Tomoda *et al.*, 1999). Theoretically, the detection of cytoplasmic p27 in both LLnL- and LMB-treated cells (Figure 4, B and D) could reflect accelerated p27 export, impaired p27 import, or impaired proteolysis of exported protein. To test this, the effects of both LMB and LLnL on nuclear p27 export were assayed (Figures 5, A-C). MCF-7 cells were grown on glass slides and were transfected with a vector encoding wild-type p27 linked to a yellow fluorescence protein (YFPp27WT). Export of YFPp27WT from the nuclei of digitonin-permeabilized cells was assayed as in Figure 2A. A progressive reduction in nuclear YFPp27WT >30 min was quantitated by fluorescence confocal microscopy using scanning laser microscopy software (Figure 5B). The addition of LMB did not delay YFPp27WT nuclear export. Similar results were evident when export was assayed in the presence of LLnL (Figure 5, A and B). Nuclear export assays of endogenous p27 using the same method as in Figure 2B confirmed the results above, with no inhibition of p27 nuclear export evident in the presence of either LMB or LLnL (M. Connor and J.M. Slingerland, unpublished data). Thus, neither LMB nor LLnL had a measurable effect on the rate or extent of p27 nuclear export.

Because LMB did not prevent p27-CRM1 interaction in vivo or in vitro, and LMB did not inhibit nuclear export of p27 in vitro, we next assayed the effect of LMB on nuclear to cytoplasmic shuttling of p27 in vivo in heterokaryons. Heterokaryon assays were conducted in which Hela cells, transfected with either YFPp27WT or green fluorescence protein linked p53 (GFPp53) vectors, were fused to untransfected NIH 3T3 cells (Figure 5C). In the heterokaryons, the consistent appearance of YFPp27WT in the NIH 3T3 nucleus (Figure 5C, white arrow) indicated that the YFPp27 was being exported from the Hela cell nucleus. Pretreatment with 50 ng/ml LMB for 2 h and cycloheximide for 30 min before heterokaryon fusion had no effect on p27 shuttling (Figure 5C, p27, -LMB, and +LMB). All heterokaryons showed p27 shuttling in the absence of LMB, and 95% of the heterokaryons pretreated with LMB displayed p27 shuttling. In contrast, as shown by Stommel *et al.* (1999), the export of GFPp53 from the Hela cell nucleus was inhibited by LMB, with 90% of the heterokaryons showing shuttling without LMB, and only 25% showing shuttling in the presence of LMB (Figure 5C, p53 -LMB versus +LMB).

Having shown that neither LLnL nor LMB appears to affect p27 export, the cytoplasmic accumulation of p27 after treatment with either drug could reflect impaired p27 nuclear import. Thus, we assayed the effect of these drugs on nuclear import of p27. After a 60-min incubation with 4 μg/μl cytosolic proteins and an ATP regenerating system, recombinant His-p27 was imported into the nuclei of digitonin-permeabilized cells (Figure 5D, 60 min). No import occurred at 4°C, in the absence of ATP and cytosol (M. Connor and J.M. Slingerland, unpublished data), or in the presence of WGA (Figure 5D). Neither LMB nor LLnL impaired His-p27 nuclear import. Thus, LMB and LLnL do not impair either p27 import or export as measured by these assays, and the appearance of cytoplasmic p27 after treat-

ment with these drugs is consistent with delayed degradation of exported protein.

p27 Contains an Atypical NES

We identified a putative NES within the Cdk-binding domain of p27 between amino acids 32 and 45 (Figure 6A) based on the homology of leucine spacing to a cryptic NES identified in the equine infectious anemia virus (EIAV) Rev protein (Mancuso *et al.*, 1998). The spacing of the three leucines in this region of p27 is highly conserved between species.

To obtain additional evidence that amino acids 32 through 45 in p27 comprise a functional NES, we tested its ability to mediate nuclear export of an unrelated protein. For this, peptides containing the putative p27 NES (CRNLFGPVDHEELTRDLE) were coupled to FITC-labeled BSA and were microinjected into nuclei of adherent HeLa cells. As is shown in Figure 6B, a significant fraction of p27NES-FITC-BSA translocated into the cytoplasm within 45 min. In contrast, the nuclear localization of FITC-BSA remained unchanged. Although p27-NES mediated export of p27NES-FITC-BSA is not very efficient, possibly due to competing events such as the observed accumulation in nuclear speckles, or due to rate-limiting binding partners, these findings support the interpretation that amino acids 32 through 45 in p27 function as an NES.

Two leucines within this region were mutated (L41A and L45A) and effects on p27 export were examined. MCF-7 cells were transiently transfected with vectors encoding YFPp27WT or the putative NES mutant p27 linked to YFP (YFPp27NES), and nuclear export of p27 from digitonin-permeabilized cells was quantitated over time. Nuclear export of YFPp27NES was slower than that of YFPp27WT (Figure 6, B and C). The export kinetics of YFPp27WT were similar to those of the endogenous p27 in Figure 2.

Mutation of S10 But Not of T187 Affects Nuclear Export of p27

p27 contains several sites whose phosphorylation could influence its nuclear export. Ishida *et al.* (2000) recently identified serine 10 (S10) as a major phosphorylation site in G0 arrested cells. Mutation of S10 to alanine strongly inhibited p27 export (Figure 6, B and C), suggesting that phosphorylation at this site is essential for nuclear export of p27. The nuclear export of YFPp27S10D was similar to that observed for YFPp27WT (M. Connor and J.M. Slingerland, unpublished results). Because p27 degradation in late G1 involves its phosphorylation at T187 by cyclin E-cdk 2, nuclear export of YFPp27T187A was assayed. The mutation of T187 to alanine had no effect on p27 export, suggesting that phosphorylation at this site is not necessary for p27 nuclear export (Figure 6).

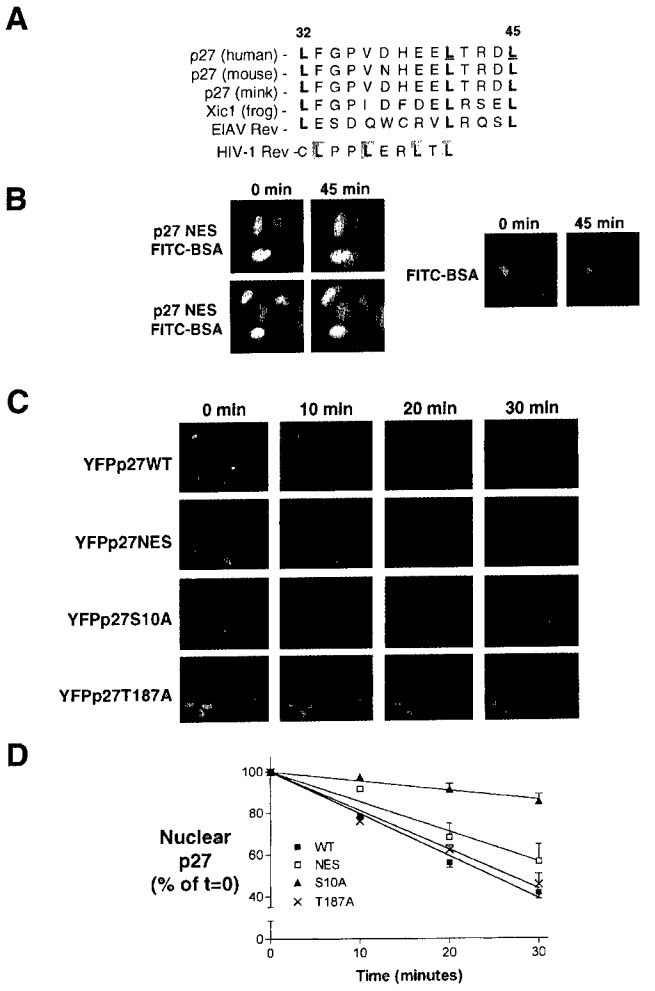

Figure 6. p27 nuclear export involves a nuclear export sequence. (A) The classical and nonclassical NES of the HIV-1Rev and EIAV Rev proteins and the sequence (amino acids 32 through 45) containing the conserved leucines in the putative p27 NES from different species are shown. (B) FITC-BSA (right panel) or FITC-BSA coupled to peptides containing the putative p27 NES (two left panels) was microinjected into the nuclei of adherant HeLa cells. Pictures at 0 and 45 min after injection were taken with identical exposure times. (C) NES mutation delays p27 export. Cells were grown on glass slides and were then transfected with YFPp27WT, YFPp27NES, YFPS10A, or YFPp27T187A. Forty-eight hours after transfection, cells were digitonin permeabilized and p27 export assayed. Nuclear export of p27 was visualized directly by photomicroscopy with a digital camera. (D) The intensity of nuclear p27 fluorescence was quantitated using Carl Zeiss Laser Scanning Software (LSM) 510 and graphed as a percentage of the maximum intensity measured at t = 0 min for each p27 allele product (p27WT, and the NES, S10A, and T187A p27 mutants).

p27-CRM1 Interaction Is Reduced by NES and S10A But Not by T187A Mutation

In vitro binding assays were conducted to test whether these p27 mutations affect p27-CRM1 interaction. To demonstrate the linearity of the p27-CRM1 binding reaction, increasing amounts of immunoprecipitated YFPp27WT (125–500 μg) were incubated with recombinant CRM1 and RanGTP, both in molar excess of p27 (Figure 7A). p27-associated CRM1 increased in proportion to the amount of input p27 in the reactions. The NES mutant p27 (L41A/L45A) bound 44% less CRM1 in vitro than did YFPp27WT (Figure 7, B and C). Thus, the reduction in p27 export conferred by the NES

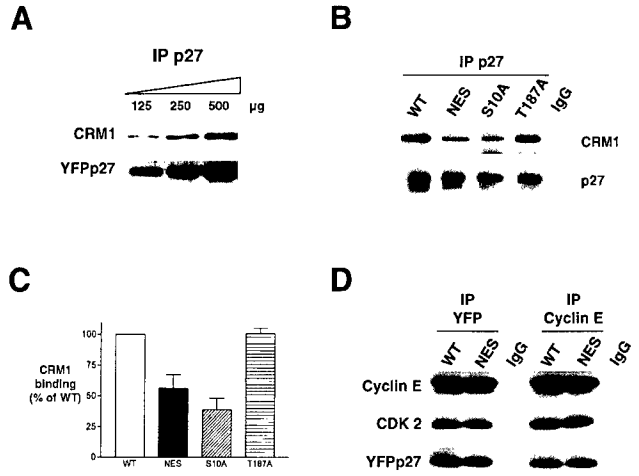

Figure 7. Effects of p27 NES mutation on CRM1- and Cyclin E-binding. (A) To show the linearity of WT p27-CRM1 binding assays, increasing amounts of heat-stable YFP-p27 (125–500 μg) were incubated with fixed amounts of CRM1 and RanGTP. p27 was immunoprecipitated and immunoblots probed for associated CRM1. (B) YFPp27 was immunoprecipitated from 300 μg of lysate from cells transfected with WT, NES, S10A, or T187A YFPp27, released from protein A beads by boiling for 10 min, and incubated with recombinant CRM1 and RanGTP. p27-complexes were probed for CRM1 and p27. CRM1 binding was corrected for differences in the amount of YFPp27 expressed in the different transfectants and graphed. (C) Graphical quantification of YFP-bound CRM1. Results represent the mean ± SEM of four independent experiments. (D) MCF-7 cells were transfected with YFPp27WT or YFPp27NES expression vectors. YFP and cyclin E immunoprecipitates were assayed for associated cyclin E, Cdk 2, or p27 by immunoblotting.

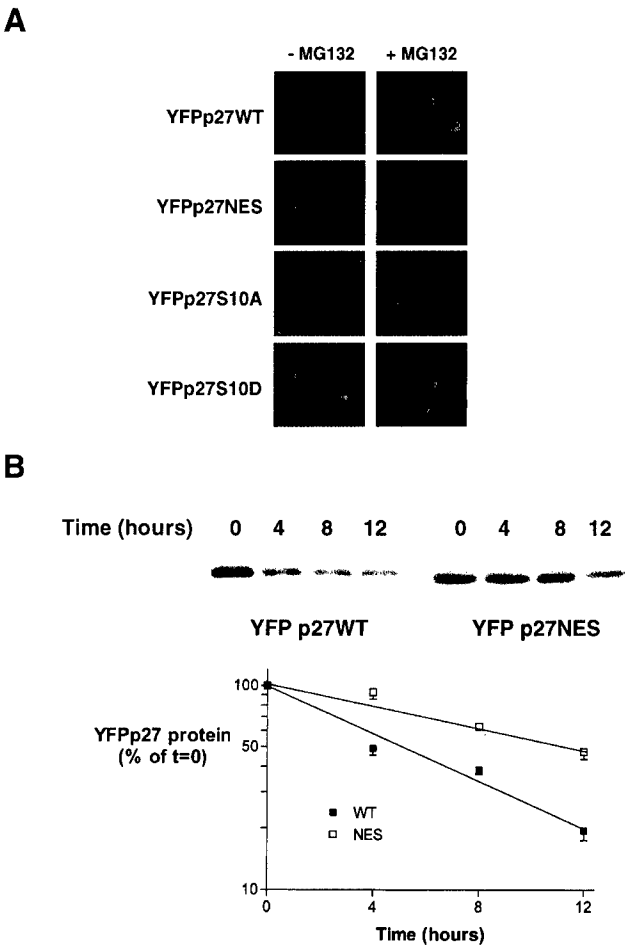

Figure 8. Effects of p27 mutation on localization and half-life. (A) Cells were grown on glass slides and transfected with either WT, NES, S10A, or S10D YFPp27 vectors for 16 h and then treated with the proteasome inhibitor MG132 (+MG132) or without (-MG132) for an additional 8 h before fixation and photomicroscopy. (B) Cells were transfected with YFPp27WT or YFPp27NES constructs and cycloheximide (100 μg/ml) was added at 48 h posttransfection. Cells were harvested 4, 8, and 12 h after cycloheximide addition, and p27 was detected by immunoblotting with YFP-specific antibody. The decay of the p27 signal is graphed as a function of time postcycloheximide addition. Linear regression curves were fitted to calculate the half-lives of each of the mutant p27 proteins using data from repeat experiments. SE bars are shown.

mutation (Figure 6) is associated with impaired binding to CRM1. Mutation of S10 to alanine also reduced p27-CRM1 binding to 40% that of p27WT. The T187A mutation of p27 did not affect either its rate of nuclear export or its binding to CRM1 (Figure 7, B and C).

Reduced Export of the p27NES Mutant Is Not Due to Decreased Cyclin E-Cdk 2 Binding

Because the p27 NES resides within its cyclin-binding domain, the increased stability of p27NES could theoretically reflect reduced binding to cyclin E-Cdk2 and thus reduced cyclin E-Cdk2-Skp2-dependent p27 proteolysis. To evaluate this, MCF-7 cells were transfected with YFPp27WT and YFPp27NES, and lysates were immunoprecipitated with either YFP or cyclin E antibodies and associated proteins were detected by immunoblotting (Figure 7D). The amount of p27NES bound to cyclin E-Cdk2 was similar to cyclin E-bound p27WT.

p27NES Shows Delayed Cytoplasmic Accumulation after Proteasome Inhibition

Cytoplasmic p27 is detected when proteasomal degradation is impaired (Figure 4B). We reasoned that if the NES mutations delay p27 export in vivo, and if some p27 undergoes cytoplasmic degradation, p27NES should show a reduced or delayed appearance in the cytoplasm after proteasome inhibition. YFPp27NES and YFPp27WT were transfected into MCF-7 cells. Newly synthesized p27 was detected exclusively in the nuclei in >90%-95% of all cell populations between 16 and 24 h posttransfection (Figure 8A, -MG132). The proteasome inhibitor, MG132 (25 μM), was added to cells at 16 h posttransfection. Direct fluorescence microscopy at intervals after MG132 addition showed a progressive cytoplasmic accumulation of p27WT, with 44% of cells showing cytoplasmic p27 by 8 h after MG132 addition (Figure 8A, + MG132). YFPp27NES showed a significant delay in redistribution of from nucleus to cytoplasm compared

with that of p27WT, with only 18% of the p27NES transfected cells displaying cytoplasmic p27 at the same 8-h time point. S10A mutation severely impaired p27 export, with only 7% of transfected cells exhibiting cytoplasmic p27 after 8 h of MG132. In contrast, the S10D mutation did not affect the accumulation of cytoplasmic p27 (Figure 8A).

Delayed Nuclear Export Is Associated with Increased p27 Protein Stability

The p27 protein half-lives ($t_{1/2}$) of p27WT and p27NES were compared by cycloheximide chase (Figure 8B). At 48 h post-transfection, both the YFPp27WT and YFPp27NES induced G0/G1 arrest as assayed by dual BrdU/propidium iodide staining and flow cytometry (M. Connor and J.M. Slingerland, unpublished data). Wild-type p27 exhibited a $t_{1/2}$ of 5.7 h. The p27NES mutant was over twice as stable as p27WT, with a $t_{1/2}$ of 11.7 h.

DISCUSSION

The reduction of p27 levels is critical for cyclin E-Cdk2 activation and G1-to-S phase progression. As cells exit G0, p27 synthesis is rapidly reduced (Hengst and Reed, 1996; Millard *et al.*, 1997) and its proteolysis is increased (Pagano *et al.*, 1995). The half-life of p27 is maximal in G0 and is reduced in asynchronous cells (Pagano *et al.*, 1995; Hengst and Reed, 1996). Indeed, in G1 and S phase cells, the p27 half-life is reduced fivefold compared with that in quiescence (Malek *et al.*, 2001). Although much is known regarding mechanisms of ubiquitin-dependent SCF^{SKP2}-mediated p27 proteolysis, the relationship between p27 localization and its degradation has been unclear.

Although molecules of up to 50 kDa can diffuse freely through nuclear pores, p27 is largely bound to multiprotein complexes. The present data suggests that both p27 import into and export from the nucleus are actively regulated. Moreover, we provide evidence that for at least part of the nuclear p27 pool, CRM1-dependent nuclear export may precede degradation. Detectable p27 is exclusively nuclear in G0 and early G1, with transient appearance in both the nucleus and cytoplasm as cells progress through G1, before its disappearance in late S phase. The dramatic increase in CRM1-p27 binding during G1 progression and the transient appearance of cytosolic p27 at the G1/S transition suggested a link between nuclear export of p27 and its degradation. Furthermore, proteasome inhibition in G1 led to the appearance of cytoplasmic p27 at a time when new p27 synthesis is minimal. The timing of cellular p27-CRM1 interaction and the observation that p27 is exported more rapidly from G1 nuclei than from G0 nuclei suggest that p27, the CRM1-ran export machinery, or both may undergo periodic posttranslational changes to facilitate p27 export in early G1. p27 phosphorylation appears to play a critical role in this process. Not only does p27 phosphorylation differ between the nucleus and cytoplasm (M. Connor and J.M. Slingerland, unpublished data), we and others have shown that the phosphorylation status of serine 10 (S10) critically regulates p27 export (Rodier *et al.*, 2001; Ishida *et al.*, 2002; Boehm *et al.*, 2002).

CRM1 mediates nuclear export by binding to a leucine-rich NES motif in the export substrate. The first NES identified was that of the HIV-1 Rev protein, and a classical NES consensus sequence has been identified based on a conserved clustering of leucine residues (Bogerd *et al.*, 1996). We propose that amino acids 32 through 45 constitute a NES for p27. The spacing of the leucine residues in this putative p27 NES is identical to that in the NES of the EIAV Rev protein. This EIAV Rev sequence is functionally homologous to the NES of the HIV-1 Rev (Mancuso *et al.*, 1998). Although the leucines in the EIAV and p27 NES are less tightly clustered than those in the HIV-1 Rev NES, their spacing is completely conserved in the p27 sequence of all known species. When a peptide comprised of amino acids 32 through 45 of p27 was linked to FITC-tagged BSA, the peptide directed export of this construct to the cytoplasm. The ability of this p27 peptide to direct the nuclear export of a heterologous protein is consistent with this sequence functioning as an NES. In control experiments, FITC-BSA without the p27 NES remained nuclear.

Mutations converting two of these three NES leucines to alanine reduced CRM1 binding, impaired export in vitro, and prolonged the half-life of the mutant p27 protein. Moreover, the p27NES mutant showed delayed and reduced accumulation in the cytoplasm after proteasome inhibition. However, mutation of these leucine residues did not affect p27 binding to cyclin E-Cdk 2, and thus, the stability of p27NES cannot be attributed to impaired cyclin E-Cdk2-mediated p27 degradation.

Nuclear export of the p27NES protein was impaired but not abolished. This may reflect the incomplete inhibition of CRM1-NES binding by these two leucine mutations, the involvement of other motifs on p27 in CRM1 binding, or the existence of another non-CRM1-dependent export mechanism for p27.

Surprisingly, LMB did not prevent the interaction between p27 and CRM1 in vitro or in vivo in LMB-treated cells. In addition, LMB did not inhibit p27 nuclear export from digitonin-permeabilized cells nor did it impair p27 export in vivo in heterokaryons. In contrast, the binding of CRM1 to cyclin D1 (Alt *et al.*, 2001) and nuclear export of another CRM1 cargo, p53 (Stommel *et al.*, 1999) were notably impaired by LMB drug concentrations that did not affect p27. LMB modifies the exportin CRM1 at C529 (Kudo *et al.*, 1999) and is thought to inhibit protein export by impairing CRM1-substrate NES interaction. The lack of effect of LMB on cellular p27-CRM1 binding and on p27 nuclear export are consistent with p27 binding to CRM1 at sites other than or in addition to the LMB-sensitive motif at C529. Our observation that classical HIV1 Rev NES peptide, which reduced cyclin D1/CRM1 interactions, did not impair p27 binding to CRM1 in vitro suggests that p27 binds to a site distinct from the classical NES-binding motif on CRM1. Transport factors have been shown to bind different cargo using slightly different binding sites (Conti and Kuriyan, 2000).

The effect of LMB on p27 export may be modulated by the binding of other proteins to the p27-CRM1 complex. The ability of LMB to interfere with CRM1 binding to Rev can be modulated by the binding of other proteins (Askjaer *et al.*, 1998). Recently, Tomoda *et al.* (2002) demonstrated that p27 nuclear export was LMB sensitive in the presence of overexpressed $p38^{Jab1}$. When the $p38^{Jab1}$ NES was mutated, effectively removing the protein from the p27-CRM1 complex, p27 export became LMB insensitive. Thus, the formation of

an export-competent p27-CRM1 complex in vivo may involve other proteins that modulate the sensitivity of p27 nuclear export to LMB. This process may show important cell type- and species-specific differences (Swanson *et al.*, 2000; Rodier *et al.*, 2001). More intensive investigation of the specific site(s) of CRM1-p27 interaction and of the composition of p27-CRM1 complexes is warranted. Nonetheless, our data raise the concern that LMB-insensitive nuclear export may not always be CRM1 independent.

LMB treatment of quiescent cells prevents their subsequent progression through G1 into S phase (M. Connor and J.M. Slingerland, unpublished data). Because p27 export from G0 nuclei is less efficient than from nuclei in early G1, the timing of LMB addition may be important when interpreting the effects of LMB on p27 export. Using p27 immunofluorescence, others have shown that LMB blocks the transient cytoplasmic accumulation of p27 that occurs when cells are released from quiescence (Rodier *et al.*, 2001; Ishida *et al.*, 2002). Since treatment with LMB in quiescence blocks G0 to G1 progression, the early G1 activation of p27 export would be compromised. Thus, the lack of cytoplasmic p27 after LMB treatment observed by others may reflect failure to exit quiescence and be an indirect effect of LMB on p27 localization.

Recent data using T187A knock-in and $Skp2^{-/-}$ mice suggest that more than one mechanism regulates p27 proteolysis, and that p27 proteolysis is T187 independent in early G1 (Hara *et al.*, 2001; Malek *et al.*, 2001). We observed that the interaction between p27 and CRM1 begins at a time in the cell cycle when both Skp2 protein levels and cyclin E-Cdk2 activities are low. Furthermore, neither nuclear export of p27 nor its binding to CRM1 are dependent on phosphorylation at T187. The present data and that of others allow the allowing model of two distinct mechanisms regulating p27 proteolysis. Mitogen-dependent phosphorylation of p27 in early/mid-G1 may lead to a reduction in p27-cyclin E-Cdk2 binding, thereby exposing the p27 NES located within the cyclin-binding domain. This would facilitate p27-CRM1 interaction and the formation of an export competent protein complex, including RanGTP. Phosphorylation at serine 10 (S10) may be a prerequisite for subsequent events that mediate CRM1 binding and nuclear export. Both our own data and that of others indicate that S10 phosphorylation is important for CRM1 binding and is required for p27 export (Rodier *et al.*, 2001; Ishida *et al.*, 2002). Binding of nucleoporins, such as Nup50, may facilitate translocation of p27 to the cytoplasm (Guan *et al.*, 2000), where it is ubiquitylated and degraded (Hara *et al.*, 2001). This early phase of export-linked p27 proteolysis appears to precede Skp2 up-regulation and cyclin E-cdk2 activation and is independent of phosphorylation on T187 by cyclin E-Cdk 2, consistent with other recent reports (Hara *et al.*, 2001; Malek *et al.*, 2001; Ishida *et al.*, 2002). This initial mechanism of p27 degradation in early G1 would allow an incremental activation of cyclin E-Cdk2. This would be followed by rapid progressive kinase activation, as activated cyclinE-Cdk2 mediates subsequent T187 phosphorylation-dependent ubiquitylation of p27 by SCF^{SKP2} and degradation in late G1 and S phase.

If an initial mechanism of titrating down p27 via nuclear export-mediated degradation is required for the efficient activation of cyclin E-Cdk2-dependent p27 proteolysis, interference with export-mediated p27 proteolysis could significantly alter the kinetics of G1 to S phase progression. The relevance of the subcellular localization of p27 to T187 phosphorylation-dependent proteolysis remains unclear. However, it has been reported that Xic1 ubiquitylation occurs in oocyte nuclei (Swanson *et al.*, 2000) and that nuclear p27 in Rat1 fibroblasts is efficiently degraded (Rodier *et al.*, 2001). This may also be the case for p27 in epithelial cells, because both nuclear and cytoplasmic p27 levels are increased after LLnL treatment.

There appear to be multiple phosphorylation sites on p27 (Ishida *et al.*, 2000; Donovan *et al.*, 2001) whose role in regulating p27 function and degradation remain unknown. Additional work is necessary to elucidate what phosphorylation events follow that of S10 in early G1 and how p27 phosphorylation may regulate its nuclear export. Although we estimate that ~20% of cellular p27 is present in CRM1 complexes in early to mid-G1, it remains unclear what proportion of the total cellular p27 is degraded after CRM1-mediated export. This may show both cell type variability and change during malignant tumor progression as a function of checkpoint losses that increase cyclin E-Cdk2 activity.

ACKNOWLEDGMENTS

We thank Geoffrey Wahl, Jayne Stommel, Ian Mattaj, Maarten Fornerod, Ralph Kehlenbach, Larry Gerace, and Alan Diehl for the reagents provided. We thank Barbara Wolff-Winiski of Novartis and Minoru Yoshida for their kind gifts of LMB. This work was supported by postdoctoral Fellowships from the Sunnybrook Trust and the U.S. Army Department of Defense Breast Cancer Research Program to M.C., and by a grant from the Canadian Breast Cancer Research Initiative (to J.M.S.). J.M.S. is supported by career awards from the Burrough's Wellcome Fund and the U.S. Army Department of Defense Breast Cancer Research Program.

REFERENCES

Adachi, M., Fukuda, M., and Nishida, E. (2000). Nuclear export of MAP kinase (ERK) involves a MAPK kinase (MEK)-dependent active transport mechanism. J. Cell Biol. *148*, 849–856.

Adam, S.A., Sterne-Marr, R., and Gerace, L. (1992). Nuclear protein import using digitonin-permeabilized cells. Methods Enzymol. *219*, 97–110.

Alt, J.R., Cleveland, J.L., Hannink, M., and Diehl, J.A. (2001). Phosphorylation-dependent regulation of cyclin D1 nuclear export and cyclin D1-dependent cellular transformation. Genes Dev. *14*, 3102–3114.

Askjaer, P., Bachi, A., Wilm, M., Bischoff, F.R., Weeks, D.L., Ogniewski, V., Ohno, M., Niehrs, C., Kjems, J., Mattaj, I.W., and Fornerod, M. (1999). RanGTP regulated interactions of CRM1 with nucleoporins and a shuttling DEADbox helicase. Mol. Cell. Biol. *19*, 6276–6285.

Askjaer, P., Jensen, T.H., Nilsson, J., Englmeier, L., and Kjems, J. (1998). The specificity of the CRM1-Rev nuclear export signal interaction is mediated by RanGTP. J.Biol.Chem. *273*, 33414–33422.

Azuma, Y., and Dasso, M. (2000). The role of Ran in nuclear function. Curr. Opin. Cell Biol. *12*, 302–307.

Boehm, M., Yoshimoto, T., Crook, M.F., Nallamshetty, S., True, A., Nabel, G.J., and Nabel, E.G. (2002). A growth factor-dependent nuclear kinase phosphorylates $p27^{Kip1}$ and regulates cell cycle progression. EMBO J. *21*, 3390–3401.

Bogerd, H.P., Fridell, R.A., Benson, R.E., Hua, J., and Cullen, B.R. (1996). Protein sequence requirements for function of the human

T-cell virus type 1 Rex nuclear export signal delineated by a novel in vivo randomization-selection assay. Mol. Cell. Biol. *16*, 4207–4214.

Cariou, S., Donovan, J.C., Flanagan, W.M., Milic, A., Bhattacharya, N., and Slingerland, J.M. (2000). Down-regulation of p21WAF1/CIP1 or p27Kip1 abrogates antiestrogen-mediated cell cycle arrest in human breast cancer cells. Proc. Natl. Acad. Sci. USA *97*, 9042–9046.

Carrano, A.C., Eytan, E., Hershko, A., and Pagano, M. (1999). SKP2 is required for ubiquitin-mediated degradation of the CDK inhibitor p27. Nat. Cell Biol. *1*, 193–199.

Cheng, M., Olivier, P., Diehl, J.A., Fero, M., Roussel, M.F., Roberts, J.M., and Sherr, C.J. (1999). The p21(Cip1) and p27(Kip1) CDK "inhibitors" are essential activators of cyclin D-dependent kinases in murine fibroblasts. EMBO J. *18*, 1571–1583.

Conti, E., and Kuriyan, J. (2000). Crystallographic analysis of the specific yet versatile recognition of distinct nuclear localization signals by karyopherin α. Struct. Fold Des. *8*, 329–338.

Donovan, J.C., Milic, A., and Slingerland, J.M. (2001). Constitutive MEK/MAPK activation leads to p27Kip1 deregulation, and antiestrogen resistance in human breast cancer cells. J. Biol. Chem. *276*, 40888–40895.

Fornerod, M., Ohno, M., Yoshida, M., and Mattaj, I.W. (1997). CRM1 is an export receptor for leucine-rich nuclear export signals. Cell *90*, 1051–1060.

Fukuda, M., Asano, S., Nakamura, T., Adachi, M., Yoshida, M., Yanagida, M., and Nishida, E. (1997). CRM1 is responsible for intracellular transport mediated by the nuclear export signal. Nature *390*, 308–311.

Ganoth, D., Bornstein, G., Ko, T.K., Larsen, B., Tyers, M., Pagano, M., and Hershko, A. (2001). The cell-cycle regulatory protein Cks1 is required for SCF(Skp2)-mediated ubiquitinylation of p27. Nat. Cell Biol. *3*, 321–324.

Gorlich, D., and Kutay, U. (1999). Transport between the cell nucleus and the cytoplasm. Annu. Rev. Cell Dev. Biol. *15*, 607–660.

Guan, T., Kehlenbach, R.H., Schirmer, E.C., Kehlenbach, A., Fan, F., Clurman, B.E., Arnheim, N., and Gerace, L. (2000). Nup50, a nucleoplasmically oriented nucleoporin with a role in nuclear protein export. Mol. Cell. Biol. *20*, 5619–5630.

Hara, T., Kamura, T., Nakayama, K., Oshikawa, K., Hatakeyama, S., and Nakayama, K.I. (2001). Degradation of p27Kip1 at the G0–G1 transition mediated by a Skp2-independent ubiquitination pathway. J. Biol. Chem. *276*, 48937–48943.

Hengst, L., Dulic, V., Slingerland, J.M., Lees, E., and Reed, S.I. (1994). A cell cycle-regulated inhibitor of cyclin-dependent kinases. Proc. Natl. Acad. Sci. USA *91*, 5291–5295.

Hengst, L., and Reed, S.I. (1996). Translational control of p27Kip1 accumulation during the cell cycle. Science *271*, 1861–1864.

Huang, T.T., Kudo, N., Yoshida, M., and Miyamoto, S. (2000). A nuclear export signal in the N-terminal regulatory domain of IκBα controls cytoplasmic localization of inactive NFκB/IκBα complexes. Proc. Natl. Acad. Sci. USA *97*, 1014–1019.

Ishida, N., Hara, T., Kamura, T., Yoshida, M., Nakayama, K., and Nakayama, K.I. (2002). Phosphorylation of $p27^{Kip\ 1}$ on serine 10 is required for its binding to CRM1 and nuclear export. J. Biol. Chem. *277*, 14355–14358.

Ishida, N., Kitagawa, M., Hatakeyama, S., and Nakayama, K. (2000). Phosphorylation at Serine 10, a major phosphorylation site of p27Kip1, increases its protein stability. J. Biol. Chem. *275*, 25146–25154.

Jin, P., Hardy, S., and Morgan, D.O. (1998). Nuclear localization of cyclin B1 controls mitotic entry after DNA damage. J. Cell Biol. *141*, 875–885.

Kehlenbach, R.H., Dickmanns, A., and Gerace, L. (1998). Nucleocytoplasmic shuttling factors including Ran and CRM1 mediate nuclear export of NFAT in vitro. J. Cell Biol. *141*, 863–874.

Kudo, N., Wolff, B., Sekimoto, T., Schreiner, E.P., Yoneda, Y., Matsumori, N., Yanagida, M., Horinouchi, S., and Yoshida, M. (1998). Leptomycin B inhibition of signal-mediated nuclear export by direct binding to CRM1. Exp. Cell Res. *242*, 540–547.

Kudo, N., Matsumori, N., Taoka, H., Fujiwara, D., Schreiner, E.P., Wolff, B., Yoshida, M., and Horinouchi, S. (1999). Leptomycin B inactivates CRM1/exportin by covalent modification at a cysteine residue in the central conserved region. Proc. Natl. Acad. Sci. USA *96*, 9112–9117.

LaBaer, J., Garrett, M.D., Stevenson, L.F., Slingerland, J.M., Sandhu, C., Chou, H.S., Fattaey, A., and Harlow, E. (1997). New functional activities for the p21 family of CDK inhibitors. Genes Dev. *11*, 847–862.

Macara, I.G. (1999). Nuclear transport: randy couples. Curr. Biol. *9*, R436–R439.

Malek, N.P., Sundberg, H., McGrew, S., Nakayama, K., Kyriakidis, T.R., and Roberts, J.M. (2001). A mouse knock-in model exposes sequential proteolytic pathways that regulate p27Kip1 in G1 and S phase. Nature *413*, 323–327.

Mancuso, V.A., Hope, T.J., Zhu, L., Derse, D., Phillips, T., and Parslow, T.G. (1998). Posttranscriptional effector domains in the rev proteins of feline immunodeficiency virus and equine infectious anemia virus. J. Virol. *68*, 1998–2001.

Mattaj, I.W., and Engimeier, L. (1998). Nucleocytoplasmic transport: the soluble phase. Annu. Rev. Biochem. *67*, 265–306.

Melchior, F., and Gerace, L. (1998). Two-way trafficking with Ran. Trends Cell Biol. *8*, 175–179.

Melchior, F. (1998). Nuclear protein import in a permeabilized cell assay. Methods Mol. Biol. *88*, 265–273.

Melchior, F., Paschal, B., Evans, J., and Gerace, L. (1993). Inhibition of nuclear protein import by nonhydrolyzable analogues of GTP and identification of the small GTPase Ran/TC4 as an essential transport factor. J. Cell Biol. *123*, 1649–1659.

Millard, S.S., Yan, J.S., Nguyen, H., Pagano, M., Kiyokawa, H., and Koff, A. (1997). Enhanced ribosomal association of p27(Kip1) mRNA is a mechanism contributing to accumulation during growth arrest. J. Biol. Chem. *272*, 7093–7098.

Montagnoli, A., Fiore, F., Eytan, E., Carrano, A.C., Draetta, G.F., Hershko, A., and Pagano, M. (1999). Ubiquitination of p27 is regulated by Cdk-dependent phosphorylation and trimeric complex formation. Genes Dev. *13*, 1181–1189.

Moore, M.S., and Blobel, G. (1993). The GTP binding protein Ran/TC4 is required for protein import into the nucleus. Nature *365*, 661–663.

Muller, D., Thieke, K., Burgin, A., Dickmanns, A., and Eilers, M. (2000). Cyclin E mediated elimination of p27 requires its interaction with the nuclear pore-associated protein mNPAP60. EMBO J. *19*, 2168–2180.

Nigg, E.A. (1997). Nucleocytoplasmic transport: signals, mechanisms and regulation. Nature *386*, 779–787.

Ohta, T., Michel, J.J., Schottelius, A.J., and Xiong, Y. (1999). ROC1, a homolog of APC11, represents a family of cullin partners with an associated ubiquitin ligase activity. Mol. Cell *3*, 535–541.

Pagano, M., Tam, S.W., Theodoras, A.M., Beer-Romero, P., Del Sal, G., Chau, V., Yew, P.R., Draetta, G.F., and Rolfe, M. (1995). Role of the ubiquitin-proteasome pathway in regulating abundance of the cyclin-dependent kinase inhibitor p27. Science *269*, 682–685.

Pines, J., and Hunter, T. (1991). Human cyclins A and B1 are differentially located in the cell and undergo cell cycle-dependent nuclear transport. J. Cell Biol. *115*, 1–17.

Pines, J., and Hunter, T. (1994). The differential localization of human cyclins A and B is due to a cytoplasmic retention signal in cyclin B. EMBO J. *13*, 3772–3781.

Polyak, K., Kato, J.Y., Solomon, M.J., Sherr, C.J., Massague, J., Roberts, J.M., and Koff, A. (1994). p27Kip1, a cyclin-Cdk inhibitor, links transforming growth factor-β and contact inhibition to cell cycle arrest. Genes Dev. *8*, 9–22.

Reynisdottir, I., and Massague, J. (1997). The subcellular locations of p15(Ink4b) and p27(Kip1) coordinate their inhibitory interactions with cdk4 and cdk2. Genes Dev. *11*, 492–503.

Rodier, G., Montagnoli, A., DiMarticullio, L., Coulombe, P., Draetta, G., Pagano, M., and Meloche, S. (2001). p27 cytoplasmic localization is regulated by phosphorylation on Ser10, and is not a prerequisite for its proteolysis. EMBO J. *20*, 6672–6682.

Sacer, S., and Dasso, M. (2000). The ran decathlon: multiple roles of Ran. J. Cell Sci. *113*, 1111–1118.

Sheaff, R.J., Groudine, M., Gordon, M., Roberts, J.M., and Clurman, B.E. (1997). Cyclin E-CDK2 is a regulator of p27Kip1. Genes Dev. *11*, 1464–1478.

Slingerland, J., and Pagano, M. (2000). Regulation of the cdk inhibitor p27 and its deregulation in cancer. J. Cell. Physiol. *183*, 10–17.

Slingerland, J.M., Hengst, L., Pan, C.H., Alexander, D., Stampfer, M.R., and Reed, S.I. (1994). A novel inhibitor of cyclin-Cdk activity detected in Transforming Growth Factor β-arrested epithelial cells. Mol. Cell. Biol. *14*, 3683–3694.

Smitherman, M., Lee, K., Swanger, J., Kapur, R., and Clurman, B.E. (2000). Characterization and targeted disruption of murine Nup50, a p27(Kip1)interacting component of the nuclear pore complex. Mol. Cell. Biol. *20*, 563156–563142.

Spruck, C., Strohmaier, H., Watson, M., Smith, A.P., Ryan, A., Krek, T.W., and Reed, S.I. (2001). A CDK-independent function of mammalian Cks1. targeting of SCF(Skp2) to the CDK inhibitor p27Kip1. Mol. Cell *7*, 639–650.

Stade, K., Ford, C.S., Guthrie, C., and Weis, K. (1997). Exportin 1 (Crm1p) is an essential nuclear export factor. Cell *90*, 1041–1050.

Stommel, J.M., Marchenko, N.D., Jimenez, G.S., Moll, U.M., Hope, T.J., and Wahl, G.M. (1999). A leucine-rich nuclear export signal in the p53 tetramerization domain: regulation of subcellular localization and p53 activity by NES masking. EMBO J. *18*, 1660–1672.

Sutterluty, H., Chatelain, E., Marti, A., Wirbelauer, C., Senften, M., Muller, U., and Krek, W. (1999). p45SKP2 promotes p27Kip1 degradation and induces S phase in quiescent cells. Nat. Cell Biol. *1*, 207–214.

Swanson, C., Ross, J., and Jackson, P.K. (2000). Nuclear accumulation of cyclin E/Cdk2 triggers a concentration-dependent switch for the destruction of p27Xic1. Proc. Natl. Acad. Sci. USA *97*, 7796–7801.

Tomoda, K., Kubota, Y., Arata, Y., Mori, S., Maeda, M., Tanaka, T., Yoshida, M., Yoneda-Kato, N., and Kato, J.Y. (2002). The cytoplasmic shuttling and subsequent degradation of p27Kip1 mediated by Jab1/CSN5 and the COP9 signalosome complex. J. Biol. Chem. *277*, 2302–2310.

Tomoda, K., Kubota, Y., and Kato, J. (1999). Degradation of the cyclin-dependent-kinase inhibitor p27Kip1 is instigated by Jab1. Nature *398*, 160–165.

Tsvetkov, L.M., Yeh, K.H., Lee, S.J., Sun, H., and Zhang, H. (1999). p27(Kip1) ubiquitination and degradation is regulated by the SCF-(Skp2) complex through phosphorylated Thr187 in p27. Curr. Biol. *9*, 661–664.

Vlach, J., Hennecke, S., and Amati, B. (1997). Phosphorylation-dependent degradation of the cyclin-dependent kinase inhibitor p27. EMBO J. *16*, 5334–5344.

Yang, J., Bardes, E.S., Moore, J.D., Brennan, J., Powers, M.A., and Kornbluth, S. (1998). Control of cyclin B1 localization through regulated binding of the nuclear export factor CRM1. Genes Dev. *12*, 2131–2143.

Zeng, Y., Hirano, K., Hirano, M., Nishimura, J., and Kanaide, H. (2000). Minimal requirements for the nuclear localization of p27Kip1, a cyclin-dependent kinase inhibitor. Biochem. Biophys. Res. Commun. *274*, 37–42.

PKB/Akt phosphorylates p27, impairs nuclear import of p27 and opposes p27-mediated G1 arrest

JIYONG LIANG[1], JUDIT ZUBOVITZ[2], TERESA PETROCELLI[1], ROUSLAN KOTCHETKOV[1], MICHAEL K. CONNOR[1], KATHY HAN[1], JIN-HWA LEE[1], SANDRA CIARALLO[1], CHARLES CATZAVELOS[3], RICHARD BENISTON[1], EDMEE FRANSSEN[4] & JOYCE M. SLINGERLAND[1,5]

[1]Molecular and Cell Biology and [2]Department of Pathology, Sunnybrook and Women's College Health Sciences Centre, [3]Department of Pathology, St. Mary's Hospital, McGill University, Montreal, Quebec [4]Division of Clinical Epidemiology and Biostatistics and [5]Medical Oncology, Toronto Sunnybrook Regional Cancer Centre, Toronto, Ontario, Canada
Correspondence should be addressed to J.M.S; email: jslingerland@med.miami.edu
T.P. and R.K. contributed equally to this study.

Published online: 16 September 2002, corrected online 23 September 2002 (details online) doi:10.1038/nm761

Mechanisms linking mitogenic and growth inhibitory cytokine signaling and the cell cycle have not been fully elucidated in either cancer or in normal cells. Here we show that activation of protein kinase B (PKB)/Akt contributes to resistance to antiproliferative signals and breast cancer progression in part by impairing the nuclear import and action of p27. Akt transfection caused cytoplasmic p27 accumulation and resistance to cytokine-mediated G1 arrest. The nuclear localization signal of p27 contains an Akt consensus site at threonine 157, and p27 phosphorylation by Akt impaired its nuclear import *in vitro*. Akt phosphorylated wild-type p27 but not p27T157A. In cells transfected with constitutively active Akt^{T308DS473D} (PKB^{DD}), p27WT mislocalized to the cytoplasm, but p27T157A was nuclear. In cells with activated Akt, p27WT failed to cause G1 arrest, while the antiproliferative effect of p27T157A was not impaired. Cytoplasmic p27 was seen in 41% (52 of 128) of primary human breast cancers in conjunction with Akt activation and was correlated with a poor patient prognosis. Thus, we show a novel mechanism whereby Akt impairs p27 function that is associated with an aggressive phenotype in human breast cancer.

Cell-cycle deregulation is a hallmark of cancer. Loss of cytokine-mediated G1 arrest may confer an advantage during malignant progression. Resistance to the antiproliferative effects of transforming growth factor-β (TGF-β) often occurs despite intact TGF-β signaling and such cells may manifest resistance to multiple inhibitory cytokines, suggesting underlying alterations in cell-cycle controls[1,2].

Cyclin-dependent kinases (cdks) are regulated by cyclin binding, phosphorylation and by two families of cdk inhibitors[3]. G1 progression is governed by D-type and E-type cyclin-cdk complexes. The inhibitors of cdk4 (INK4) family includes p15^{INK4B} and the kinase inhibitor protein (KIP) family comprises p21^{Cip1}, p27^{Kip1} and p57^{Kip2} (ref. 4). In addition to inhibition of cyclin E-cdk2, p21 and p27 also facilitate assembly and activation of cyclin D-cdks in early G1 (refs. 5,6).

p27^{Kip1} was first identified as a mediator of TGF-β1-induced G1 arrest[7–9]. TGF-β induces expression of the gene encoding *p15^{INK4B}*. p15^{INK4B} binds and inhibits cdk4 facilitating dissociation of p27 and cyclin D1 from cyclin D1–cdk4–p27 complexes and p27 binds and inhibits cyclin E-cdk2, leading to G1 arrest[10–12]. p27 also mediates G1 arrest induced by IL-6 (ref. 13). p27 is a nuclear protein whose frequent deregulation in human cancers may confer resistance to antiproliferative signals. In cMyc or MAPK activated cancer-derived lines, cyclin D1–cdk4/6 complexes sequester p27, and cyclin E-cdk2-inhibition is impaired[14–16]. cMyc inhibits p15 induction by TGF-β (ref. 17) and may also induce a factor that inactivates p27[18]. In up to 50% of human cancers, reduced p27 protein is associated with a poor prognosis[19]. In some tumors, p27 is mislocalized to the cytoplasm[19,20], however; the mechanism and significance of this has not been elucidated.

In human cancers, constitutive activation of phosphoinositol 3′ kinase (PI3K) and its effector PKB/Akt arise through oncogenic receptor tyrosine kinase activation, *Ras* activation, mutational loss of *PTEN*, or through activating mutation of the PI3K effector, protein kinase B (PKB)/Akt (hereafter termed Akt) itself[21,22]. Akt can increase cyclin D1 levels[23] and downregulate p27 by increasing p27 proteolysis[24] or repressing p27 expression through Akt phosphorylation of a forkhead transcription factor[25]. However, in most cancers, reduced p27 does not result from transcriptional silencing[19].

Here we show that Akt causes resistance to cytokine-mediated G1 arrest. p27 phosphorylation by Akt impairs its nuclear import and leads to cytoplasmic p27 accumulation. In human breast cancers, cytoplasmic mislocalization of p27 is associated with Akt activation, loss of differentiation and poor patient outcome.

Activation of Akt in lines resistant to G1 arrest by TGF-β

Ras has been shown to confer TGF-β resistance. While investigating mechanisms of TGF-β resistance, we found that two TGF-β

resistant lines showed activation of the Ras effector, PI3K-Akt pathway. TGF-β causes G1 arrest of normal 184 human mammary epithelial cells (HMECs) and of the early stage melanoma line, WM35, but not the resistant 184A1L5^R or advanced melanoma-derived line, WM239 (Fig. 1*a* and *b*). Resistant lines showed increased Akt activation (Akt-P) (Fig. 1*c* and *d*). Total Akt was similar in sensitive and resistant HMECs. Akt levels were somewhat higher in WM239 than WM35. PTEN loss contributed to Akt activation in WM239 (Fig. 1*d*).

The increased PI3K-Akt activity in 184A1L5^R and WM239 was linked to their TGF-β resistance, as partial PI3K inhibition restored TGF-β responsiveness. In 184A1L5^R, low concentrations of the PI3K inhibitor, LY294002 (10–12.5 μM) modestly reduced the S phase fraction (% S) but allowed continued proliferation, with a profile similar to that of 184 cells (Fig. 2*a*). Although TGF-β alone had little effect, 10 μM LY294002 together with TGF-β caused G1 arrest of 184A1L5^R (Fig. 2*a*). In TGF-β-resistant WM239, LY294002 at a concentration that did not independently inhibit proliferation led to G1 arrest when combined with TGF-β (data not shown).

Because inhibition of cyclin E-cdk2 by p27 contributes to G1 arrest by TGF-β, cyclin E1 complexes were assayed in 184AIL5^R. A low dose of LY294002 (10 μM) inhibited Akt activity (Fig. 2*b*). LY294002 did not change p27 protein levels in HMECs (Fig. 2*b*), but modestly increased cyclin E1–bound p27 and partly inhibited cyclin E1-cdk2 activity (Fig. 2*b*). TGF-β and LY294002 together increased further cyclin E1–bound p27 and inhibited cyclin E1-cdk2 causing G1 arrest. Thus, attenuation of P13K activity restored cyclin E1-cdk2 inhibition by p27 and G1 arrest by TGF-β.

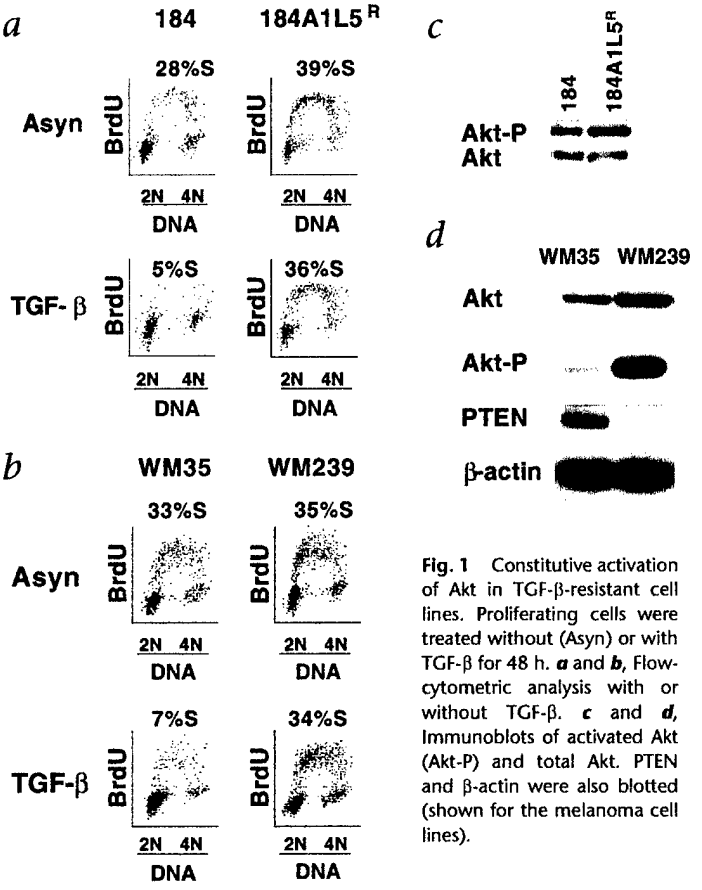

Fig. 1 Constitutive activation of Akt in TGF-β-resistant cell lines. Proliferating cells were treated without (Asyn) or with TGF-β for 48 h. ***a*** and ***b***, Flow-cytometric analysis with or without TGF-β. ***c*** and ***d***, Immunoblots of activated Akt (Akt-P) and total Akt. PTEN and β-actin were also blotted (shown for the melanoma cell lines).

Akt inhibits responsiveness to antiproliferative cytokines

184 and WM35 cells were transfected with a constitutively active Akt^{T308DS473D} (PKB^{DD})[26,27] or empty vector (E). Transfectants showed increased Akt protein and activity (Fig. 2*c*). PKB^{DD}-transfected lines were resistant to G1 arrest by TGF-β (shown for WM35^{PKBDD})

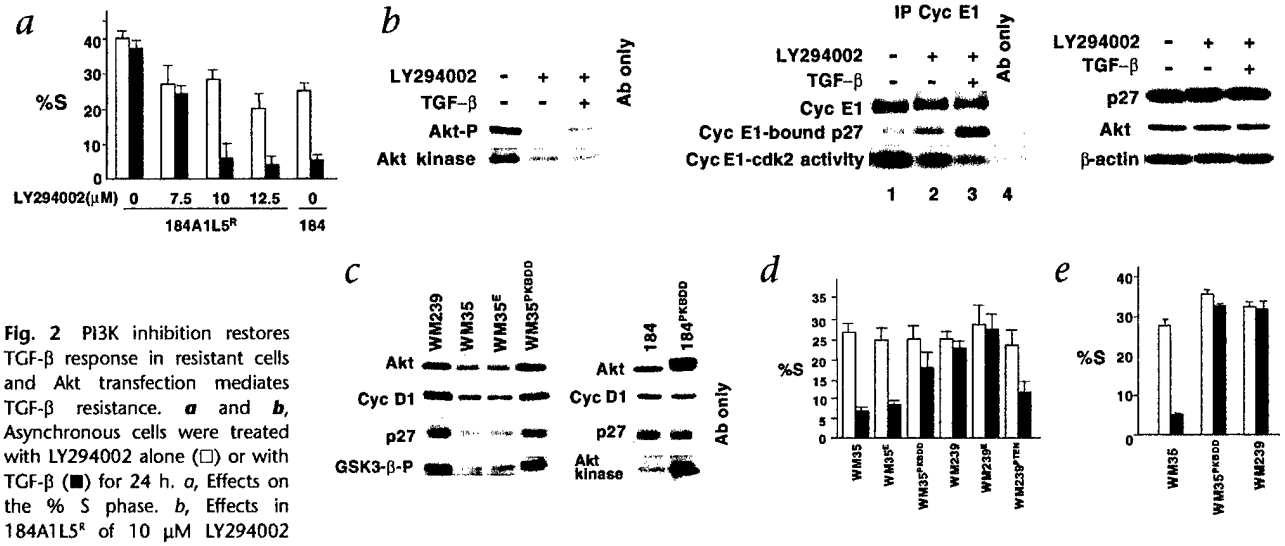

Fig. 2 PI3K inhibition restores TGF-β response in resistant cells and Akt transfection mediates TGF-β resistance. ***a*** and ***b***, Asynchronous cells were treated with LY294002 alone (□) or with TGF-β (■) for 24 h. *a*, Effects on the % S phase. *b*, Effects in 184A1L5^R of 10 μM LY294002 with or without TGF-β on Akt-P levels, Akt kinase activities, cyclin E1-association with p27 and cyclin E-cdk2 activities. Lane 4 shows the antibody only control for the left and middle panels. Total Akt, p27 and β-actin levels are shown in the right panel. ***c–e***, The indicated cells were transformed with PKB^{DD}, PTEN or empty vector (E). *c*, Ectopic expression of PKB^{DD} was shown by western blot (Akt) and Akt activity confirmed by blotting for phosphorylation of the Akt substrate, GSK3-β (GSK3-β-P) or by Akt kinase assays (Akt kinase). Levels of p27 and cyclin D1 are shown. *d* and *e*, Flow cytometric analysis of parental and transfected cells treated with (■) or without (□) TGF-β (*d*) and without (□) or with (■) IL-6 (*e*) for 48 h.

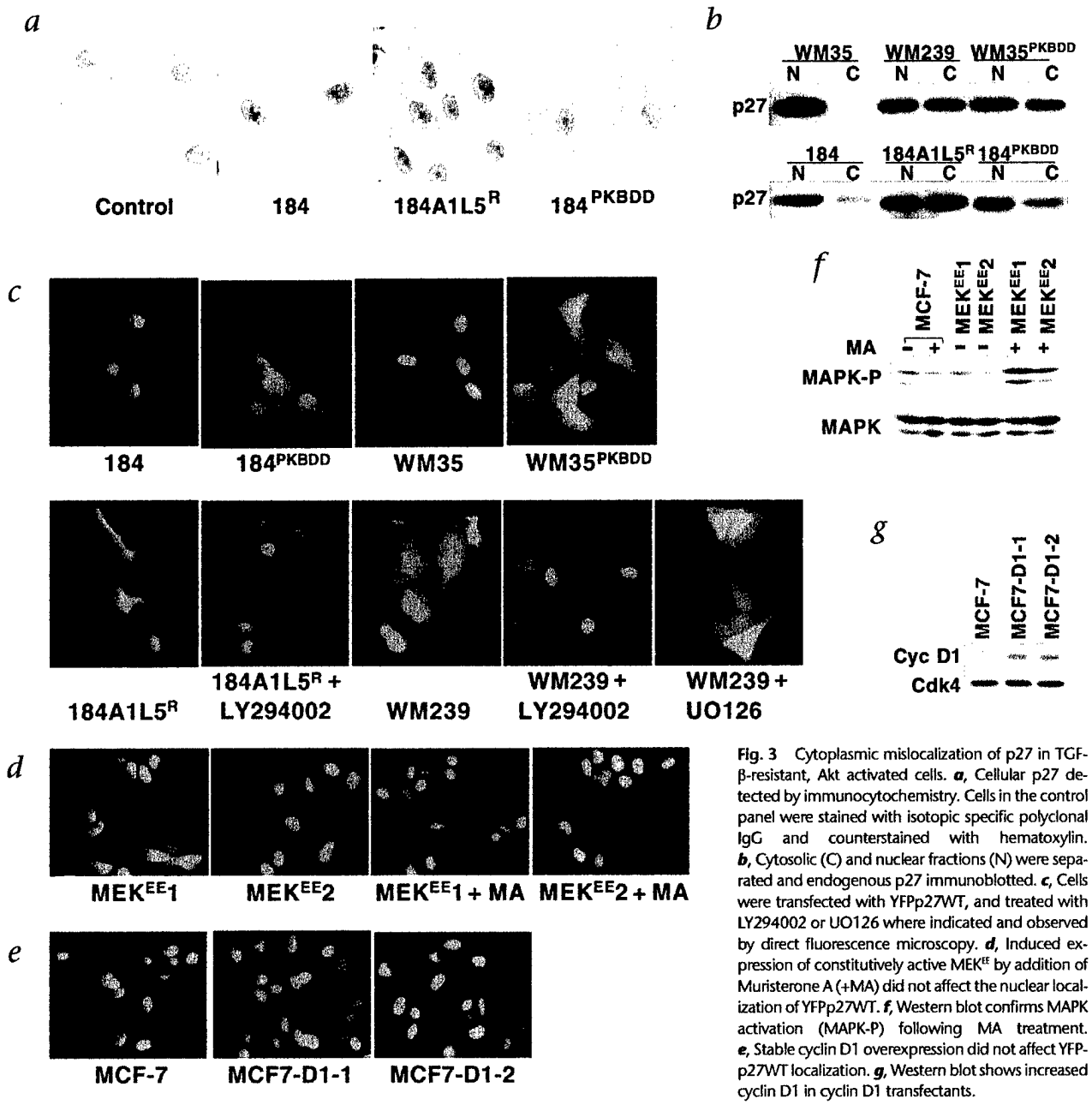

Fig. 3 Cytoplasmic mislocalization of p27 in TGF-β-resistant, Akt activated cells. ***a***, Cellular p27 detected by immunocytochemistry. Cells in the control panel were stained with isotopic specific polyclonal IgG and counterstained with hematoxylin. ***b***, Cytosolic (C) and nuclear fractions (N) were separated and endogenous p27 immunoblotted. ***c***, Cells were transfected with YFPp27WT, and treated with LY294002 or UO126 where indicated and observed by direct fluorescence microscopy. ***d***, Induced expression of constitutively active MEK^{EE} by addition of Muristerone A (+MA) did not affect the nuclear localization of YFPp27WT. ***f***, Western blot confirms MAPK activation (MAPK-P) following MA treatment. ***e***, Stable cyclin D1 overexpression did not affect YFP-p27WT localization. ***g***, Western blot shows increased cyclin D1 in cyclin D1 transfectants.

(Fig. 2*d*). Moreover, PKB^{DD} transfection also conferred resistance to G1 arrest by IL-6 (Fig. 2*e*). In WM239, transfection of PTEN restored TGF-β sensitivity (Fig. 2*d*).

Akt causes cytoplasmic mislocalization of p27

Because Akt impairs the nuclear localization of some of its substrates[28], we assayed if Akt activation affected p27 localization. Cellular p27 was predominantly nuclear in 184 HMEC. $184A1L5^R$ and 184^{PKBDD} cells showed both nuclear and cytoplasmic p27 (Fig. 3*a*). Increased cytoplasmic p27 in WM239 and $WM35^{PKBDD}$, and in $184A1L5^R$ and 184^{PKBDD} compared with WM35 and 184, respectively, was confirmed by immunoblotting of fractionated cell lysates (Fig. 3*b*).

Transfected fluorescent-tagged wild-type p27 (YFPp27WT) was exclusively nuclear in most 184 and WM35 cells (Fig. 3*c* and Supplementary Table A online). YFPp27WT-transfected $184A1L5^R$ and WM239 showed increased cytoplasmic p27. LY294002 restored the predominantly nuclear localization of YFPp27WT in TGF-β-resistant $184A1L5^R$ and WM239 cells (Fig. 3*c*). In 184^{PKBDD} and $WM35^{PKBDD}$, transfected YFPp27WT showed increased cytoplasmic localization, similar to that in $184A1L5^R$ and WM239.

In contrast to effects of LY294002, treatment of WM239 cells with the MEK inhibitor, UO126, did not result in redistribution of p27 from cytoplasm to nucleus. Moreover, in two independent cell lines, inducible overexpression of constitutively activated MEK (MEK^{EE}) and MAPK activation did not cause

cytoplasmic mislocalization of p27 (Fig. 3*d* and *f*). Thus, in this culture model, MAPK activation is neither necessary nor sufficient for cytoplasmic mislocalization of p27. As both Akt and MAPK activation can increase cyclin D1 levels, we tested the effect of cyclin D1 transfection on p27 localization. Cyclin D1 overexpression did not mediate cytoplasmic localization of p27 (Fig. 3*e* and *g*).

Akt binds and phosphorylates cellular p27^{Kip1}

A minimal consensus motif has been defined for Akt (ref. 29). p27 contains a putative Akt consensus sequence between amino acids 152 and 157 (RKRPAT). Immunoprecipitated cellular Akt could phosphorylate recombinant p27 directly *in vitro* as well as the known Akt substrate, histone H2B. p27T157A, generated by replacing the T157 with alanine, was much less efficiently phosphorylated by Akt (Fig. 4*a*). Thus, T157 is identified as a putative Akt phosphorylation site in p27. The inability of Akt to phosphorylate p27T157A is not due to loss of Akt binding as both endogenous p27 and ectopically expressed p27WT and p27T157A coprecipitated with activated cellular Akt-P (Fig. 4*b*).

To demonstrate that phosphorylation of p27 by Akt can occur in cells, p27 immunoprecipitates from asynchronous and LY294002-treated WM239 and MCF-7 cells were immunoblotted with a phospho-specific antibody against the Akt phosphorylation consensus motif (P-Akt substrate antibody). Immunoreactivity with this antibody demonstrated cellular p27 phosphorylation at the Akt consensus motif in asynchronous cells. This was inhibited by LY294002 (Fig. 4*c*).

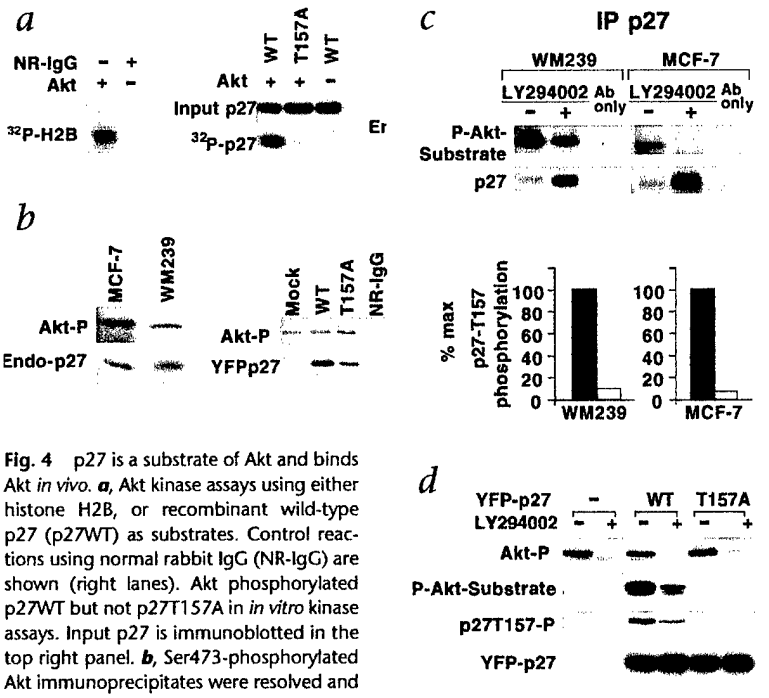

Fig. 4 p27 is a substrate of Akt and binds Akt *in vivo*. ***a***, Akt kinase assays using either histone H2B, or recombinant wild-type p27 (p27WT) as substrates. Control reactions using normal rabbit IgG (NR-IgG) are shown (right lanes). Akt phosphorylated p27WT but not p27T157A in *in vitro* kinase assays. Input p27 is immunoblotted in the top right panel. ***b***, Ser473-phosphorylated Akt immunoprecipitates were resolved and immunoblotted to show Akt-P and associated endogenous cellular p27 (left panel) or transfected YFPp27WT and YFPp27T157A (right panel). ***c***, Cellular p27 shows reactivity with antibody specific for the phosphorylated Akt consensus motif. While p27 levels are increased by LY294002, reactivity with the phospho-Akt substrate antibody (P-Akt substrate) is diminished. Lower graph: ■, without LY294002; □, with LY294002. ***d***, WM239 cells were transfected with YFPp27WT or YFPp27T157A and then treated with or without LY294002 for 20 hours. The top band shows Akt-P. YFPp27 was immunoblotted with antibodies to P-Akt substrate, anti-p27T157-P and total p27.

In normal 184 HMECs, Akt-P is minimal in G0 and increases rapidly when cells enter early G1 (data not shown). Using an antibody specific for T157-phosphorylated p27 generated by Viglietto *et al.*, we showed that cellular T157 phosphorylated p27 was minimal in G0 and the relative amount of T157 phosphorylated p27 over total p27 rose by 1.8-fold within 4 hours of exit from quiescence (data not shown). Densitometric analysis of p27T157-P and total p27 blots showed that the relative amount of T157 phosphorylated over total p27 was two-fold higher in proliferating WM239 than in WM35 (data not shown). Thus, activation of Akt *in vivo* is associated with increased T157 phosphorylation of p27 in both normal HMECs and in tumor-derived cells.

To provide further evidence for p27 phosphorylation by Akt *in vivo*, WM239 cells were transfected with either YFPp27WT or YFPp27T157A and treated with 20 μM LY294002. LY294002 markedly reduced reactivity of YFPp27WT with the antibody to the phosphorylated Akt consensus motif (P-Akt substrate) and the p27T157-P antibody. p27T157A showed minimal reactivity with the antibody to phosphorylated Akt substrate and none to anti-p27T157-P (Fig. 4*d*).

p27T157A is nuclear in cells with constitutive Akt

T157 is located within the nuclear localization signal (NLS) of p27[30,31]. Phosphorylation of the NLS regulates nuclear localization of many proteins[32]. To assay whether the potential for T157 phosphorylation might influence p27 localization, WM35^{PKBDD} cells were transfected with YFPp27WT, YFPp27T157A and YFPp27T157D (Fig. 5*a* and Supplementary Table B online). While approximately 30% of YFPp27WT and YFPp27T157D expressing cells showed both nuclear and cytoplasmic p27, YFPp27T157A was nuclear.

WM239 cells, whose Akt is constitutively activated, were transiently transfected with either YFPp27WT or YFPp27T157A. Flow cytometric analysis of YFP positive cells at 20 hours post-transfection revealed that the cell-cycle inhibitory function of p27WT was significantly impaired, while p27T157A retained G1 inhibitory function in WM239 (Fig. 5*b*). Equal expression of YFPp27WT and YFPp27T157A was demonstrated (Fig. 4*d*, lower). In contrast, YFPp27WT and YFPp27T157A both caused G1 arrest in 184 HMECs and WM35 cells lacking constitutive Akt activation (data not shown). Thus p27 phosphorylation by Akt impairs its G1 inhibitory function.

Phosphorylation by Akt impairs nuclear import of p27

p27 nuclear import was assessed by the incubation of His-tagged p27 (His-p27) with digitonin permeabilized MCF-7 cells. Nuclei and supernatant fractions were then immunoblotted for His-p27. Prior reaction of recombinant His-p27WT with cellular Akt kinase impaired nuclear import of p27. His-p27T157A showed a faster rate of import than His-p27WT, and His-p27T157D protein showed essentially no nuclear import above that of negative controls (reactions carried out at 4 °C, without ATP or in the presence of wheat germ agglutinin) (Fig. 5*c*). These data suggest that cytoplasmic p27 in Akt activated cells results from impaired p27 nuclear import.

Cytoplasmic p27 and activated Akt in human breast cancers

p27 protein levels and localization were reviewed in 128 primary breast cancers previously stained for p27 by immunohistochemistry[33]. Levels of p27 were scored as high (>50%) or low (≤50%) tumor nuclei staining as previously described[33]. While normal breast ductal epithelium and lymphocytes and a majority of tumors (Fig. 6*a*) showed exclusively nuclear p27, 42% (52/128) of the breast cancers showed either nuclear and cytoplasmic or predominantly cytoplasmic p27 (Fig. 6*b* and *c*). Of cancers with reduced p27 levels, 44% (31/70) showed cytoplasmic p27, while 36% (21/58) of tumors with high p27 levels showed cytoplasmic p27. p27 protein levels and cytoplasmic p27 mislocalization were not statistically correlated (chi square analysis, $P = 0.3542$).

Cytoplasmic p27 was not correlated with menopausal, nodal or ER/PR status. Tumors with high levels of exclusively nuclear p27 (N only; p27 >50% nuclei positive) (Fig. 6*a*) were almost all well differentiated or of low grade, whereas tumors with high levels of p27 but cytoplasmic localization (N+C; p27 >50%) (Fig. 6*b*) were more poorly differentiated ($P < 0.001$ on χ^2 analysis) (Supplementary Table C). The Kaplan–Meier curve in Fig. 6*d* shows the influence of p27 localization on patient survival. Fig. 6*e* shows that for each level of p27 staining (high, >50% nuclei positive or low, ≤50% nuclei positive), when p27 is seen in the cytoplasm (N+C) rather than in the nucleus alone (N), patient survival is worse. These data were statistically significant for overall survival ($P = 0.05$, Wilcoxon test) (Fig. 6*e*) and for disease-free survival ($P = 0.003$, data not shown). Patients with breast cancers with high levels of exclusively nuclear p27 (N only; p27 >50%) had the best outcome, whereas the worst survival was seen in those with reduced p27 levels and detectable cytoplasmic p27 (N+C; ≤50%, $P = 0.02$, Log-rank test) (Fig. 6*f*).

53 breast cancers were stained with phospho-Akt antibody (Fig. 6*a–c*, right). Normal quiescent breast acini, lymphocytes and stroma showed no Akt-P staining. None of 23 tumors with exclusively nuclear p27 showed Akt activation, whereas 28/30 tumors with cytoplasmic p27 showed phospho-Akt reactivity. Detection of cytoplasmic p27 in human breast tumors was highly statistically significantly associated with Akt activation (χ^2, $P < 0.001$).

Discussion

This study suggests that constitutive activation of the PI3K-Akt pathway mediates TGF-β resistance. TGF-β- and IL-6-sensitive cells were rendered resistant by ectopic Akt activation. Akt activity was increased in 184A1L5^R and WM239 cells. Moreover, *PTEN* transfection into WM239 cells, and inhibition of PI3K by LY294002 in TGF-β-resistant cells restored p27 binding and inhibition of cyclin E-cdk2 and G1 arrest by TGF-β.

Whereas PI3K signaling can inhibit p27 transcription or accelerate p27 degradation in different cell types, we show that Akt can bind p27 and phosphorylate T157. Akt phosphorylated p27WT but not p27T157A *in vitro*. Moreover, the reactivity of cellular and transfected p27 with phospho-Akt substrate and p27T157-P antibodies was strongly reduced by Akt inhibition following LY294002 treatment. The p27T157A showed minimal reactivity with the antibody to phosphorylated Akt substrate and none with anti-p27T157-P. Cellular p27 phosphorylation at T157 increased in normal HMECs in association with Akt activation as cells moved from G0 into G1. Moreover, T157 phosphorylation of p27 was two-fold higher in PTEN-deficient WM239 than in WM35 cells, indicating that T157 of p27 is a putative Akt site *in vivo*.

T157 lies within the nuclear localization signal of p27 (NLS, aa 153–166)[30,31]. Our data indicate that an Akt-dependent pathway regulates p27 localization. Although the T157A mutation may facilitate p27 import irrespective of PKB, phosphorylation at this site appears to inhibit nuclear import of p27. Cells with activated Akt showed cytoplasmic p27. LY294002 treatment or expression of p27T157A in cells with activated Akt restored nuclear p27 localization. Moreover, Akt^{DD} transfection led to cytoplasmic mislocalization of p27. p27 phosphorylation by Akt impaired nuclear p27 import *in vitro*. Phosphorylation within or near the NLS has been shown to inhibit nuclear import of other proteins[32]. Thus, as for other Akt substrates p21, and some forkhead transcription factors (refs. 28,34), in cancers the constitutive p27 phosphorylation by Akt may cause a relative cytoplasmic sequestration of p27. This would limit the p27 available to bind to and inhibit cyclin E-cdk2, compromising the arrest response to antiproliferative factors such as TGF-β and IL-6. In contrast, in normal HMECs, T157 phosphorylation of p27 ac-

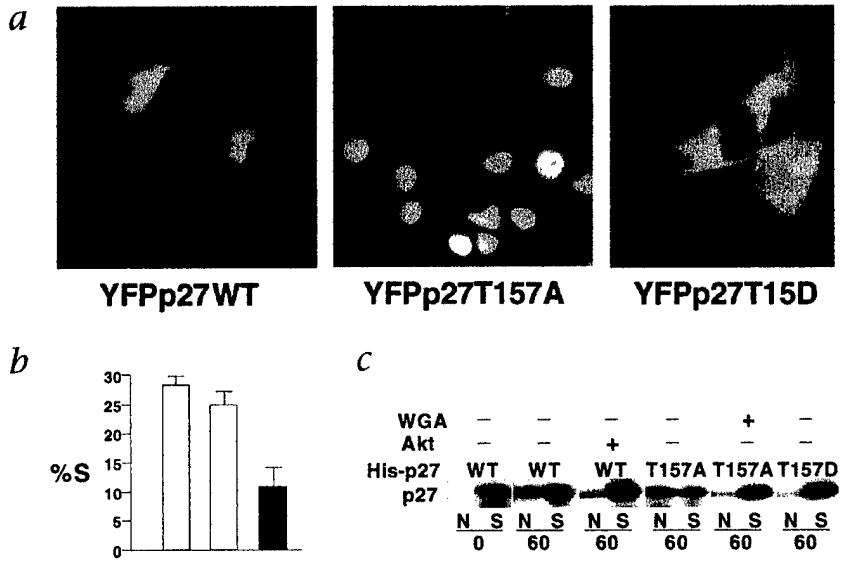

Fig. 5 T157 phosphorylation impairs nuclear import of p27. ***a***, p27 localization following transfection of the indicated p27 alleles into WM35 cells expressing PKB^{DD} (WM35^{PKBDD}). ***b***, WM239 cells were transiently transfected with YFPp27 alleles and the cell-cycle profile of YFP-positive cells analyzed by flow cytometry. □, untransfected; ▩, wild-type; ■, T157A-transfected. ***c***, p27 nuclear import was assessed by the addition of His-tagged p27 (His-p27) to digitonin permeabilized cells for 60 minutes (60) and nuclear, (N), and supernatant, (S), fractions were immunoblotted for p27. Input His-p27WT is shown in the left-most lane (t=0 minutes). Pre-treatment of His-p27WT with cellular Akt (+Akt) impaired p27 import. Import reactions for His-p27T157A (T157A) and His-p27T157D (T157D) are shown. Import of T157A was abolished by addition of wheat germ agglutinin (+ WGA).

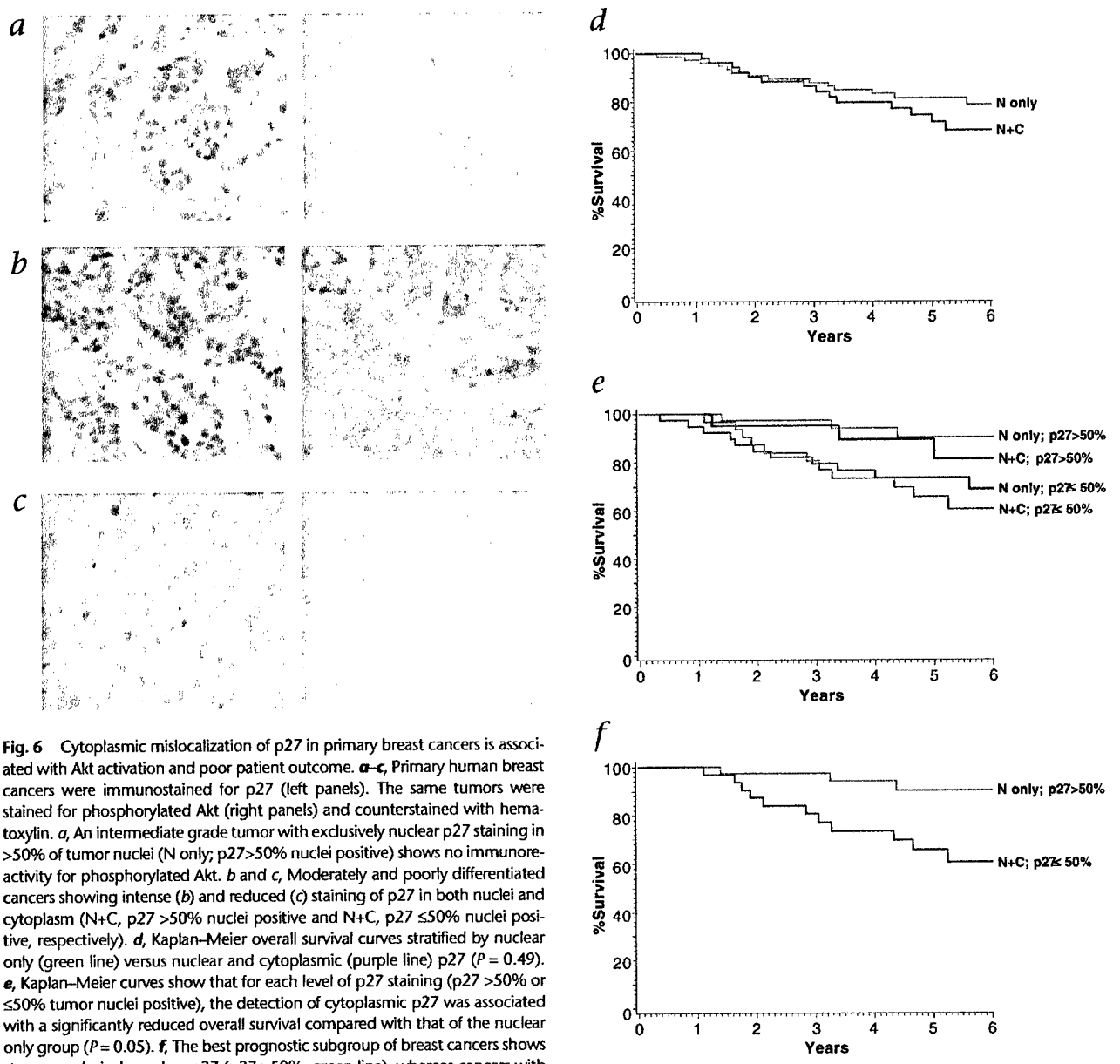

Fig. 6 Cytoplasmic mislocalization of p27 in primary breast cancers is associated with Akt activation and poor patient outcome. ***a–c***, Primary human breast cancers were immunostained for p27 (left panels). The same tumors were stained for phosphorylated Akt (right panels) and counterstained with hematoxylin. *a*, An intermediate grade tumor with exclusively nuclear p27 staining in >50% of tumor nuclei (N only; p27>50% nuclei positive) shows no immunoreactivity for phosphorylated Akt. *b* and *c*, Moderately and poorly differentiated cancers showing intense (*b*) and reduced (*c*) staining of p27 in both nuclei and cytoplasm (N+C, p27 >50% nuclei positive and N+C, p27 ≤50% nuclei positive, respectively). ***d***, Kaplan–Meier overall survival curves stratified by nuclear only (green line) versus nuclear and cytoplasmic (purple line) p27 ($P = 0.49$). ***e***, Kaplan–Meier curves show that for each level of p27 staining (p27 >50% or ≤50% tumor nuclei positive), the detection of cytoplasmic p27 was associated with a significantly reduced overall survival compared with that of the nuclear only group ($P = 0.05$). ***f***, The best prognostic subgroup of breast cancers shows strong, exclusively nuclear p27 (p27 >50%; green line), whereas cancers with both reduced levels and cytoplasmic mislocalization of p27 (p27 ≤50%; red line) have the lowest survival ($P = 0.02$).

companies the periodic activation of Akt and may regulate normal p27 function in early G1. It is noteworthy that the PKB consensus sequence in p27 is imperfect and shows some species variation. While PKB may phosphorylate p27 at this site in humans, the possibility that other kinases phosphorylate T157 cannot be excluded.

PKB^{DD} transfection increased cyclin D1 levels in the $WM35^{PKBDD}$ but not in 184^{PKBDD}, but p27 was mislocalized to cytoplasm in both cell types. PKB^{DD} mediated cytoplasmic p27 mislocalization does not result from increased cyclin D1, since cyclin D1 overexpression did not cause cytoplasmic sequestration of p27 in our assays.

Whereas many reports have shown the importance of accelerated p27 proteolysis causing reduced p27 in human cancer[19], only one study showed an effect of cytoplasmic p27 on outcome in esophageal cancer[20]. Patient data in which p27 loss and p27 localization are analyzed together with respect to disease outcome have not been published to date. Here, we demonstrate that Akt-mediated phosphorylation of p27 in its NLS impairs its nuclear import *in vitro* and show that cytoplasmic p27 localization is linked to Akt activation in human breast cancer *in vivo* and is associated with reduced patient survival.

Three independent reports (including this study) demonstrate cytoplasmic p27 in up to 40% of primary human breast cancers in association with activated Akt (Viglietto *et al.* and Shin *et al.* in this issue). Serine 473-phosphorylated Akt was not detected in normal breast epithelium and Akt-P staining showed greater intensity in invasive than in non-invasive tumor areas within individual breast cancers (unpublished data). Tumors with uniquely

nuclear p27 localization showed no Akt activation.

Although Akt can inhibit p27 gene expression by targeting the forkhead transcription factors[25] and loss of *PTEN* may lead to accelerated p27 proteolysis[24], this seems to be cell-type dependent and may require additional changes in signaling pathways. LY294002 increased p27 protein in the melanoma lines but not in normal HMECs. In HMECs and in human breast cancers, Akt activation was not always associated with p27 loss. There was no statistical correlation between cytoplasmic p27 and reduced p27 protein in primary breast cancers. Approximately the same proportion of tumors with high and low p27 scores showed cytoplasmic p27. One possible implication of this is that the processes leading to cytoplasmic p27 mislocalization and accelerated p27 proteolysis may arise independently *in vivo* and each may contribute to tumor progression.

For all levels of p27 staining, the presence of p27 in the tumor-cell cytoplasm was associated with reduced differentiation and lower disease-free survival ($P = 0.003$) and overall survival ($P = 0.05$). These data have implications for the clinical application of p27 as a prognostic factor. Taking into account the presence or absence of cytoplasmic p27 may add to the prognostic significance of reduced p27 levels. Larger studies will be needed to confirm this.

Although one report suggested that p21 phosphorylation by Akt leads to its cytoplasmic sequestration[34], two other groups confirmed that p21 is a Akt substrate, but did not observe cytoplasmic mislocalization of p21 upon Akt activation[35,36]. p21 is expressed more sporadically and at lower levels than p27 in human breast cancers and previous studies have shown conflicting results regarding the prognostic potential of p21 (ref. 37). Although mislocalization of both p21 and p27 could theoretically cooperate to promote tumor progression and a comprehensive study of p21 and p27 levels and localization would be of value, p27 may have greater potential clinical utility in cancer prognosis.

Recent reports suggest that MAPK activation accelerates p27 proteolysis[38,39]. This study, together with reports from Viglietto and Arteaga, suggest that constitutive PI3K-Akt activation contributes to oncogenesis through inhibition of nuclear p27 import and hence its cdk inhibitory function. Cytoplasmic mislocalization of p27 worsens the prognosis associated with reduced p27 levels in breast cancer supporting the relevance of these mechanisms to human tumorigenesis. Although some tumors show evidence of both accelerated p27 proteolysis and cytoplasmic localization, others show only one or the other. In human cancers, mutational activation of *Ras* and loss of the tumor suppressor *PTEN* are not infrequent[21,22]. Overexpression of receptor tyrosine kinases (RTKs), such as Her2, can also activate PI3K-Akt in human breast and other cancers[40]. As both PI3K and MAPK are downstream of RTK-Ras, it will be of interest to determine what additional pathways direct RTK signaling to mediate either p27 proteolysis or cytoplasmic mislocalization in some breast cancers, while in others both coexist.

Akt phosphorylates proteins involved in signal transduction, apoptosis and gene expression[40], and increasing evidence suggests that this pathway contributes importantly to cell-cycle regulation. Although this pathway affects multiple cell-cycle effectors, including cyclin D and p21, the present study, together with those of Arteaga and Viglietto, define a novel mechanism linking Akt activation with impaired nuclear p27 import and p27 deregulation in human cancer.

Methods

Cell culture. Finite life span HMEC strain 184 (ref. 41) and immortalized 184AIL5[R] (ref. 12), MCF-7 cells[42] and WM35 and WM239 lines[43] were cultured as described. Cells were treated with 10 ng/ml TGF-β.

Plasmids, site-directed mutagenesis and transfection. The retroviral pBABE vector or pBABE constructs carrying the constitutively activated, hemagglutinin (HA)-tagged $PKB^{T308D/S473D}$ (PKB^{DD})[26,27] or wild-type PTEN were transfected as described[26]. Human wild-type p27 cDNA (p27WT) was inserted into the pIND vector. T157 of p27 was replaced with alanine (p27T157A) or aspartic acid (p27T157D) by site-directed mutagenesis using a QuickChange site-directed mutagenesis kit (Strategene, Loyola, California). The WT and mutant p27 cDNAs were then subcloned into pEYFP-C1 vector (Clontech, Palo Alto, California) encoding an N-terminal yellow-green variant of the *Aequorea victoria* green fluorescent protein (YFP). The YFP-p27 vectors were transfected using LipofectAMINE/PLUS reagents (Invitrogen, Carlsbad, California) according to the manufacturer's protocol. Muristerone A (MA) inducible MEK^{EE} expression was achieved in MCF-7 cells using the 2-plasmid system from Invitrogen. In the absence of MA, cells showed basal MAPK activity. MA increased MAPK-P in 2 different MEK^{EE} inducible lines. pRC-CMV-cyclin D1 (provided by P. Hinds) was transfected into MCF-7 cells to generate cyclin D1–overexpressing cell lines.

Intracellular localization of p27. HMECs were EGF-depleted for 48 h and endogenous p27 detected by immunocytochemistry as described[33]. Nuclear cytoplasmic fractionation was carried out by digitonin-permeabilization as described[44]. Nuclei were isolated by centrifugation and the supernatant containing the cytosolic fraction collected. Equal cell volumes of nuclear and cytoplasmic lysates were assayed for p27 by immunoblotting. The nuclear protein, RCC1, was blotted as a fractionation control. YFP-tagged p27 expression was detected by direct fluorescence microscopy of transfected cells. Photographs were taken at ×400 magnification using an Empix digital camera and 'CoolSnap' (Photomajics, Pittsfield, Massachusetts) software.

Nuclear import assays. Import assays were carried out as described[44]. MCF-7 cells were digitonin permeabilized and isolated nuclei incubated with cytosolic proteins (4 μg/μl), an ATP-regenerating system and recombinant his-tagged WT, T157A or T157D p27 for 60 min at 21 °C. Nuclear and supernatant fractions were then separated by centrifugation and immunoblotted for His-p27. Where indicated, His-p27WT was reacted *in vitro* with cellular Akt before import assays. Pre-incubation with wheat germ agglutinin (200 μg/ml) abolished active p27 import.

Flow cytometry. Cells were pulse-labeled with 10 μM bromodeoxyuridine (BrdU), stained with anti-BrdU-conjugated FITC (Becton Dickinson, Mountain View, California) and propidium iodide and cell-cycle data acquired as described[12].

Recombinant protein, affinity purification and kinase assays. The p27WT, p27T157A and p27T157D cDNAs were subcloned into pET28a. Recombinant His-p27 was purified on nickel-agarose beads. An antibody against serine 473 (Ser473) phosphorylated Akt (ref. 26) was used to assay Akt activation by immunoblotting. For assays of Akt activity, Akt was immunoprecipitated from 1 mg cell lysates and reacted with GSK-3-α as substrate using an Akt kinase kit (New England Biolabs, Beverly, Massachusetts). Akt kinase assays were also carried out using either 5 μg histone-H2B or 10 μg recombinant His-p27 as substrates as described[45]. Cyclin E1-dependent kinase activity was assayed and quantified as described[9].

Antibodies and immunoblotting. Antibodies to Akt, GSK-3-β, phospho-Akt, phospho-GSK3-β (Thr21) were obtained from New England Biolabs; to p27 (C-19) and cdk2 from Santa Cruz Biotechnology (San Cruz, California); to p27 (DCS72) from Neomarkers (Fremont, California); to p27 from Transduction Labs (Lexington, Kentucky); to β-actin from Sigma (Oakville, Ontario). Cyclin E1 antibodies (mAbs E12 and E172) were obtained from E. Harlow. Antiphospho-Akt-substrate antibody was from New England Biolabs. The antibody specific for T157-phosphorylated p27 was generated and provided by G. Viglietto. Cells were lysed in ice-cold NP-40 lysis buffer and immunoblotted as described[12].

Patient population and statistical methods. The population studied was a group of 128 patients who underwent surgery for non-metastatic primary breast cancer between 1986 and 1992 at the Sunnybrook Health Sciences Center. This study was approved by the Research Ethics Board of the hospital. Kaplan-Meier survival and disease free survival curves were generated using nuclear p27 score and nuclear versus nuclear and cytoplasmic p27 as strata. Log-rank, Wilcoxon and –2log (LR) were used to assess significance. The association between discrete variables was tested using the χ^2 test.

Immunohistochemistry. Paraffin sections of tumor blocks were stained for p27 as described[33] using monoclonal p27 antibody (Transduction Labs, Lexington, Kentucky) diluted 1:1000 (0.25 μg/ml) in PBS or for phospho-Akt using the phospho-Akt (Ser473) antibody (NEB) diluted 1:200. Sections were counterstained with hematoxylin. The degree and localization of p27 staining was scored independently by two pathologists (C.C. and J.Z.) and J.M.S. as described[33]. Tumors showing both nuclear and cytoplasmic or exclusively cytoplasmic p27 in at least 35% of cells were scored 'N+C'. Tumors with exclusively nuclear p27 were scored as nuclear only (N only). Phospho-Akt was scored by J.Z. and J.M.S.

Note: Supplementary information is available on the Nature Medicine website.

Acknowledgments

We thank J. Woodgett for PKB/Akt vectors; M. Stampfer for 184 and 184A1L5^R cells; K. Robertson for construction of the p27T157A mutant; L. Attisano, D. Dumont and J. Woodgett for helpful discussions; and C. Arteaga and G. Viglietto for sharing unpublished results. J.L. is supported by a US Army DOD Breast Cancer Research Program Pre-Doctoral Award. J.M.S. is supported by the US Army DOD Breast Cancer Research Program, the Burrough's Wellcome Fund and by Cancer Care Ontario. This work was funded by the Canadian Breast Cancer Research Initiative.

Competing interests statement

The authors declare that they have no competing financial interests.

RECEIVED 17 APRIL; ACCEPTED 14 AUGUST 2002

1. Donovan, J. & Slingerland, J. Transforming growth factor-β and breast cancer: Cell cycle arrest by transforming growth factor-β and its disruption in cancer. *Breast Cancer Res.* **2**, 116–124 (2000).
2. Kretzschmar, M. Transforming growth factor-β and breast cancer: Transforming growth factor-β/SMAD signaling defects and cancer. *Breast Cancer Res.* **2**, 107–115 (2000).
3. Sherr, C.J. G1 phase progression: Cycling on cue. *Cell* **79**, 551–555 (1994).
4. Sherr, C.J. & Roberts, J.M. CDK inhibitors: Positive and negative regulators of G1-phase progression. *Genes Dev.* **13**, 1501–1512 (1999).
5. LaBaer, J. *et al.* New functional activities for the p21 family of CDK inhibitors. *Genes Dev.* **11**, 847–862 (1997).
6. Cheng, M. *et al.* The p21(Cip1) and p27(Kip1) CDK 'inhibitors' are essential activators of cyclin D-dependent kinases in murine fibroblasts. *EMBO J.* **18**, 1571–1583 (1999).
7. Koff, A., Ohtsuki, M., Polyak, K., Roberts, J.M. & Massague, J. Negative regulation of G1 in mammalian cells: Inhibition of cyclin E-dependent kinase by TGF-β. *Science* **260**, 536–539 (1993).
8. Polyak, K. *et al.* p27^{Kip1}, a cyclin-Cdk inhibitor, links transforming growth factor-β and contact inhibition to cell cycle arrest. *Genes Dev.* **8**, 9–22 (1994).
9. Slingerland, J.M. *et al.* A novel inhibitor of cyclin-Cdk activity detected in transforming growth factor β-arrested epithelial cells. *Mol. Cell. Biol.* **14**, 3683–3694 (1994).
10. Hannon, G.J. & Beach, D. p15^{INK4B} is a potential effector of TGF-β-induced cell cycle arrest. *Nature* **371**, 257–261 (1994).
11. Reynisdottir, I., Polyak, K., Iavarone, A. & Massague, J. Kip/Cip and Ink4 Cdk inhibitors cooperate to induce cell cycle arrest in response to TGF-β. *Genes Dev.* **9**, 1831–1845 (1995).
12. Sandhu, C. *et al.* Transforming growth factor β stabilizes p15^{INK4B} protein, increases p15^{INK4B}-cdk4 complexes and inhibits cyclin D1/cdk4 association in human mammary epithelial cells. *Mol. Cell Biol.* **17**, 2458–2467 (1997).
13. Florenes, V.A. *et al.* Interleukin-6 dependent induction of the cyclin dependent kinase inhibitor p21WAF1/CIP1 is lost during progression of human malignant melanoma. *Oncogene* **18**, 1023–1032 (1999).
14. Bouchard, C. *et al.* Direct induction of cyclin D2 by Myc contributes to cell cycle progression and sequestration of p27. *EMBO J.* **18**, 5321–5333 (1999).
15. Cheng, M., Sexl, V., Sherr, C.J. & Roussel, M.F. Assembly of cyclin D-dependent kinase and titration of p27^{Kip1} regulated by mitogen-activated protein kinase kinase (MEK1). *Proc. Natl. Acad. Sci. USA* **95**, 1091–1096 (1998).
16. Perez-Roger, I., Kim, S.H., Griffiths, B., Sweing, A. & Land, H. Cyclins D1 and D2 mediate Myc-induced proliferation via sequestration of p27^{Kip1} and p21^{Cip1}. *EMBO J.* **18**, 5310–5320 (1999).
17. Warner, B.J., Blain, S.W., Seoane, J. & Massague, J. Myc downregulation by transforming growth factor β required for activation of the p15^{INK4B} G1 arrest pathway. *Mol. Cell Biol.* **19**, 5913–5922 (1999).
18. Vlach, J., Hennecke, S., Alevizopoulos, K., Conti, D. & Amati, B. Growth arrest by the cyclin-dependent kinase inhibitor p27^{Kip1} is abrogated by c-Myc. *EMBO J.* **15**, 6595–6604 (1996).
19. Slingerland, J. & Pagano, M. Regulation of the cdk inhibitor p27 and its deregulation in cancer. *J. Cell Physiol.* **183**, 10–17 (2000).
20. Singh, S.P. *et al.* Loss or altered subcellular localization of p27 in Barrett's associated adenocarcinoma. *Cancer Res.* **58**, 1730–1735 (1998).
21. Bos, J.L. Ras oncogenes in human cancer: A review. *Cancer Res.* **49**, 4682–4689 (1989).
22. Di Cristofano, A. & Pandolfi, P.P. The multiple roles of PTEN in tumor suppression. *Cell* **100**, 387–390 (2000).
23. Diehl, J.A., Cheng, M., Roussel, M.F. & Sherr, C.J. Glycogen synthase kinase-3β regulates cyclin D1 proteolysis and subcellular localization. *Genes Dev.* **12**, 3499–3511 (1998).
24. Sun, H. *et al.* PTEN modulates cell cycle progression and cell survival by regulating phosphatidylinositol 3,4,5,trisphosphate and Akt/protein kinase B signaling pathway. *Proc. Natl. Acad. Sci. USA* **96**, 6169–6204 (1999).
25. Medema, R.H., Kops, G.J., Bos, J.L. & Burgering, B.M. AFX-like Forkhead transcription factors mediate cell-cycle regulation by Ras and PKB through p27^{Kip1}. *Nature* **404**, 782–787 (2000).
26. Alessi, D.R. *et al.* Mechanism of activation of protein kinase B by insulin and IGF-1. *EMBO J.* **15**, 6541–6551 (1996).
27. Wang, Q. *et al.* Protein kinase B/Akt participates in GLUT4 translocation by insulin in L6 myoblasts. *Mol. Cell Biol.* **19**, 4008–4018 (1999).
28. Muslin, A.J. & Xing, H. 14-3-3 proteins: Regulation of subcellular localization by molecular interference. *Cell Signal* **12**, 703–709 (2000).
29. Obata, T. *et al.* Peptide and protein library screening defines optimal substrate motifs for AKT/PKB. *J. Biol Chem.* **275**, 36108–36115 (2000).
30. Reynisdottir, I. & Massague, J. The subcellular locations of p15(Ink4b) and p27(Kip1) coordinate their inhibitory interactions with cdk4 and cdk2. *Genes Dev.* **11**, 492–503 (1997).
31. Zeng, Y., Hirano, K., Hirano, M., Nishimura, J. & Kanaide, H. Minimal requirements for the nuclear localization of p27^{Kip1}, a cyclin-dependent kinase inhibitor. *Biochem. Biophys. Res. Commun.* **274**, 37–42 (2000).
32. Jans, D.A. & Hubner, S. Regulation of protein transport to the nucleus: Central role of phosphorylation. *Physiol Rev.* **76**, 651–685 (1996).
33. Catzavelos, C. *et al.* Decreased levels of the cell-cycle inhibitor p27^{Kip1} protein: Prognostic implications in primary breast cancer. *Nature Med.* **3**, 227–230 (1997).
34. Zhou, B.P. *et al.* Cytoplasmic localization of p21$^{Cip1/WAF1}$ by Akt-induced phosphorylation in HER-2/neu-overexpressing cells. *Nature Cell Biol.* **3**, 245–252 (2001).
35. Rossig, L. *et al.* Akt-Dependent Phosphorylation of p21^{Cip1} regulates PCNA binding and proliferation of endothelial cells. *Mol. Cell Biol.* **21**, 5644–5657 (2001).
36. Li, Y., Dowbenko, D. & Lasky, L.A. AKT/PKB phosphorylation of p21Cip/WAF1 enhances protein stability of p21$^{Cip/WAF1}$ and promotes cell survival. *J. Biol. Chem.* **277**, 11352–11361 (2002).
37. Tsihlias, J., Kapusta, L. & Slingerland, J. The prognostic significance of altered cyclin-dependent kinase inhibitors in human cancer. *Annu. Rev. Med.* **50**, 401–423 (1999).
38. Yang, H.-Y., Zhou, B.P., Hung, M.-C. & Lee, M.-H. Oncogenic signals of HER-2/neu in regulating the stability of the cyclin-dependent kinase inhibitor p27. *J. Biol. Chem.* **275**, 24735–24739 (2000).
39. Donovan, J.C., Milic, A. & Slingerland, J.M. Constitutive MEK/MAPK activation leads to p27^{Kip1} deregulation and antiestrogen resistance in human breast cancer cells. *J. Biol. Chem.* **276**, 40888–40895 (2001).
40. Coffer, P.J., Jin, J. & Woodgett, J.R. Protein kinase B (c-Akt): A multifunctional mediator of phosphatidylinositol 3-kinase activation. *Biochem. J.* **335**, 1–13 (1998).
41. Stampfer, M. Isolation and growth of human mammary epithelial cells. *J. Tissue Cult. Methods* **9**, 107–115 (1985).
42. Soule, H.D., Vazguez, J., Long, A., Albert, S. & Brennan, M. A human cell line from a pleural effusion derived from a breast carcinoma. *J. Natl. Cancer Inst.* **51**, 1409–1416 (1973).
43. Herlyn,M. Human melanoma: Development and progression. *Cancer Metastasis Rev.* **9**, 101–112 (1990).
44. Adam, S.A., Sterne-Marr, R. & Gerace, L. Nuclear protein import using digitonin-permeabilized cells. *Methods Enzymol.* 97–110 (1992).
45. Franke, T.F. *et al.* The protein kinase encoded by the Akt proto-oncogene is a target of the PDGF-activated phosphatidylinositol 3-kinase. *Cell* **81**, 727–736 (1995).